ARTICLES
https://doi.org/10.1038/s41591-021-01404-8

nature medicine

Check for updates

Locoregional infusion of HER2-specific CAR T cells in children and young adults with recurrent or refractory CNS tumors: an interim analysis

Nicholas A. Vitanza[1,2]✉, Adam J. Johnson[1,3], Ashley L. Wilson[1,3], Christopher Brown[3,4], Jason K. Yokoyama[1,3], Annette Künkele[5,6,7], Cindy A. Chang[8], Stephanie Rawlings-Rhea[1,3], Wenjun Huang[1,3], Kristy Seidel[3], Catherine M. Albert[2,7], Navin Pinto[2,7], Juliane Gust[9,10], Laura S. Finn[11,12], Jeffrey G. Ojemann[13], Jason Wright[14], Rimas J. Orentas[1,2], Michael Baldwin[1], Rebecca A. Gardner[1,2,3], Michael C. Jensen[2,3,15,16] and Julie R. Park[2,3,7,16]

Locoregional delivery of chimeric antigen receptor (CAR) T cells has resulted in objective responses in adults with glioblastoma, but the feasibility and tolerability of this approach is yet to be evaluated for pediatric central nervous system (CNS) tumors. Here we show that engineering of a medium-length CAR spacer enhances the therapeutic efficacy of human erb-b2 receptor tyrosine kinase 2 (HER2)-specific CAR T cells in an orthotopic xenograft medulloblastoma model. We translated these findings into BrainChild-01 (NCT03500991), an ongoing phase 1 clinical trial at Seattle Children's evaluating repetitive locoregional dosing of these HER2-specific CAR T cells to children and young adults with recurrent/refractory CNS tumors, including diffuse midline glioma. Primary objectives are assessing feasibility, safety and tolerability; secondary objectives include assessing CAR T cell distribution and disease response. In the outpatient setting, patients receive infusions via CNS catheter into either the tumor cavity or the ventricular system. The initial three patients experienced no dose-limiting toxicity and exhibited clinical, as well as correlative laboratory, evidence of local CNS immune activation, including high concentrations of CXCL10 and CCL2 in the cerebrospinal fluid. This interim report supports the feasibility of generating HER2-specific CAR T cells for repeated dosing regimens and suggests that their repeated intra-CNS delivery might be well tolerated and activate a localized immune response in pediatric and young adult patients.

CAR T cells have demonstrated clinical efficacy against hematopoietic malignancies[1], but the utility of CAR T cells for pediatric CNS tumors is still being explored. For over a decade, HER2 has been developed as a target for CAR T cells[2–5]. HER2 is an appealing target for treatment of CNS tumors as it is not expressed on normal CNS tissue but is expressed across a spectrum of biologically diverse CNS tumors, including ependymoma, glioblastoma and medulloblastoma—the most common childhood CNS embryonal tumor—as well as on CNS cancer stem cells[4–8]. Monoclonal antibodies to HER2, such as trastuzumab (Herceptin), have shown clinical success against multiple HER2$^+$ tumor types[9–11]. However, the blood–brain barrier of the CNS, and the lower HER2 expression in CNS tumors relative to breast cancer, limit the application of HER2-targeting antibodies against CNS tumors[12] and support the investigation of cellular therapies delivered directly to the tumor site. Based on phase 1 clinical trial data showing the safety and feasibility of repetitive locoregional CAR T cell administration to treat patients with glioblastoma[13–15], we aimed to develop HER2-specific CAR T cells, incorporating principles made evident in CD19CAR testing[1], that could be advanced to clinicals trials for locoregional treatment of CNS tumors in children and young adults.

We show that the spacer length enhances the preclinical activity of HER2-specific CAR T cells, highlighting the importance of target epitope position for activity of CAR T cells. Based on our in vitro and in vivo preclinical work, we advanced a medium-length (M) spacer HER2CAR into the phase 1, single-institution clinical trial BrainChild-01 (NCT03500991), which evaluates the repeated locoregional delivery of HER2-specific CAR T cells for children with recurrent or refractory CNS tumors, including diffuse midline glioma.

We report initial feasibility, tolerability and correlative data from our initial three patients. Before opening enrollment to the broader age cohort of 1–26 years, this cohort of patients aged 15–26 years was intentionally designed for evaluation, as they could more readily

[1]The Ben Towne Center for Childhood Cancer Research, Seattle Children's Research Institute, Seattle, WA, USA. [2]Division of Pediatric Hematology/Oncology, Department of Pediatrics, University of Washington, Seattle, WA, USA. [3]Seattle Children's Therapeutics, Seattle, WA, USA. [4]Therapeutic Cell Production Core, Seattle Children's Research Institute, Seattle, WA, USA. [5]Department of Pediatric Oncology and Hematology, Charité Universitätsmedizin Berlin, corporate member of Freie Universität Berlin, Humboldt Universität zu Berlin, and Berlin Institute of Health, Berlin, Germany. [6]German Cancer Consortium (DKTK), Heidelberg, Germany. [7]Center for Clinical and Translational Research, Seattle Children's Research Institute, Seattle, WA, USA. [8]Office of Animal Care, Seattle Children's Research Institute, Seattle, WA, USA. [9]Department of Neurology, University of Washington, Seattle, WA, USA. [10]Center for Integrative Brain Research, Seattle Children's Research Institute, Seattle, WA, USA. [11]Department of Laboratories, Seattle Children's Hospital, Seattle, WA, USA. [12]Department of Laboratory Medicine and Pathology, University of Washington School of Medicine, Seattle, WA, USA. [13]Division of Neurosurgery, Department of Neurological Surgery, Seattle Children's Hospital, Seattle, WA, USA. [14]Department of Radiology, Seattle Children's Hospital, Seattle, WA, USA. [15]Department of Bioengineering, University of Washington, Seattle, WA, USA. [16]These authors contributed equally: Michael C. Jensen, Julie R. Park. ✉e-mail: nicholas.vitanza@seattlechildrens.org

self-report any neurologic changes. These patients received multiple locoregional CAR T cell infusions in the outpatient setting at dose level (DL) 1 and DL2 without any dose-limiting toxicities (DLTs). In addition, these patients experienced post-treatment symptoms (and one imaged patient had radiographic evidence) consistent with treatment-mediated localized CNS immune activation. These clinical findings correlated temporally with high concentrations of cytokines CXCL10 (C-X-C motif chemokine ligand 10) and CCL2 (C-C motif chemokine ligand 2) in patient cerebrospinal fluid (CSF) and serum samples.

Results

CAR extracellular spacer length influences HER2-specific CAR T cell function. CAR T cell target engagement depends on multiple spatial parameters, such as the length and rigidity of the CAR spacer (non-antigen engaging extracellular domain); the structure and accessibility of the target; and the location of the targeted epitope, such as its distance from the cell membrane[16–19]. Previous studies underscored that CAR activity against various antigen targets is affected by spacer length, although most described and clinically relevant CARs to date contain short-length (S) spacer domains based on the CD8α or IgG4 hinge[20–23]. Given the juxtamembrane epitope location bound by trastuzumab, we tested a panel of longer CAR spacer domains in addition to the S-spacer IgG4 hinge via the incorporation of the IgG4 CH3 or CH2-CH3 domains onto the HER2CAR, creating medium-length (M) or long-length (L) spacers, respectively (Extended Data Fig. 1a). The use of an IgG4 scaffold, well described in CAR design, provides flexibility to the scFv and modularity to CAR extracellular length[24,25]. Mutations in the IgG4 hinge also promote inter-disulfide bonds and CAR stability[24,25]. We transduced bulk CD8$^+$ T cells with second-generation 41BB-CD3ζ CARs containing variable extracellular spacer lengths (Methods). We found that the M- and L-spacer HER2CARs elicited similar levels of specific lysis and cytokine production (IFNγ and TNFα) against the HER2$^+$ medulloblastoma cell lines D283 and Med411FH but not against HER2$^-$ D341 cells (Extended Data Fig. 2a–c). Of note, S-spacer HER2CAR T cells failed to lyse or produce cytokines against HER2$^+$ targets.

We next sought to confirm S-spacer HER2CAR functionality and analyze the effect of target epitope position on CAR activity. We fused a minimal HER2 epitope to the N-terminal end of the extracellular domain of CD19 and evaluated S-spacer HER2CAR recognition of target cells expressing this HER2–CD19 fusion construct (Extended Data Fig. 2d). Moving the location of the HER2 epitope, as per HER2t–CD19t, rescued S-spacer CAR activity to levels similar to or greater than that observed for M- or L-spacer CARs (Extended Data Fig. 2e,f). These data demonstrate that the juxtamembrane position of the HER2 epitope targeted by the HER2CAR precludes S-spacer functionality and that bioactive CARs specific to this epitope require extended spacer domains.

We created medulloblastoma xenografts using D283 eGFP:ffluc cells stereotactically implanted into the cerebral hemisphere (Methods). Seven days later, mice were treated with a single intratumoral dose of untransduced control (mock) versus S-, M- or long mutant (Lmut)-spacer HER2CAR-expressing CD8$^+$ T cells (the Lmut spacer is an L-spacer modified at two key residues to support in vivo function[16]; Methods). Mice treated with mock and S-spacer HER2CAR T cells failed to respond to treatment, as evidenced by a rapid increase in bioluminescent signal, necessitating euthanasia approximately 21 d after tumor inoculation (Extended Data Fig. 3a–c). In contrast, all mice treated with the M-spacer and a subset of the mice treated with the Lmut-spacer HER2CAR T cells regressed to baseline biophotonic tumor signal after T cell injection. The therapeutic benefit of the M- and Lmut-spacer lasted up to the defined experimental endpoint of more than 90 d after tumor engraftment, with the M-spacer outperforming all groups (M-spacer versus mock ($P=0.0035$), S-spacer ($P=0.0021$) and Lmut-spacer ($P=0.025$); Extended Data Fig. 3a,d).

To replicate progressive disease, we used D283 eGFP:ffluc cells in an orthotopic intracerebroventricular model of leptomeningeal metastatic spread. The M-spacer HER2CAR significantly reduced tumor growth in both the head and spine and prolonged median survival by 44.1 d (Extended Data Fig. 3e,f). Expression of IL-2, incorporated to enhance T cell function and proliferation in D283 eGFP:ffluc tumor cells, further prolonged median survival to the endpoint of the study (Extended Data Fig. 3e). HER2CAR-treated mice removed from the study were euthanized for predetermined routine signs of tumor progression (that is, lethargy, hunching and weight loss), and none of the mice exhibited other neurotoxicity. These experiments were performed with CD8$^+$ HER2CAR T cells before adopting mixed CD4$^+$:CD8$^+$ CAR T cell products in our clinical trials; however, a repeated preclinical study with a mixed CD4$^+$:CD8$^+$ HER2-specific CAR T cell product revealed similar efficacy in vivo, with increased median survival compared to mock T cells ($P=0.002$; Extended Data Fig. 4a–c).

BrainChild-01: clinical trial design and initial three patients. Considering the frequency of HER2 positivity of pediatric CNS tumors[7], the clinical tolerability of the HER2 antibody trastuzamb[9], our institutional success conducting CAR T cell trials with highly potent anti-tumor activity[1] and the preclinical efficacy of our M-spacer HER2-specific CAR T cells, Seattle Children's opened the phase 1 single-institution clinical trial called BrainChild-01 (NCT03500991). This trial locoregionally delivers HER2-specific CAR T cells to children and young adults with recurrent or refractory HER2$^+$ CNS tumors (Fig. 1a–c). Locoregional administration, as opposed to systemic intravenous dosing, was chosen based on results from our preclinical testing and independent preclinical confirmation of superior efficacy compared to systemic dosing[26,27]. Patients were separated into two arms: delivering CAR T cells through a CNS catheter into either the tumor cavity or the ventricular system. Lymphodepletion was not performed because, in our repeated locoregional dosing algorithm, it is not feasible to continuously lymphodeplete before each infusion and because objective radiographic responses have been observed in the absence of lymphodepletion in adult CNS CAR T cell patients[14]. Within each dose regimen (DR), patients have the opportunity for intra-patient dose escalation with a maximum DL of 2 for DR1, DL3 for DR2 and DL4 for DR3.

The three BrainChild-01 patients (S001, S002 and S003) described in this initial report were enrolled on DR1 of their respective arm (Table 1). All patients had undergone three or more tumor-directed surgical procedures and had received at least one prior irradiation and at least one prior chemotherapy regimen. Before opening enrollment to ages 1–26 years, we enrolled a cohort aged 15–26 years, as they could more readily self-report any neurologic changes. The first three patients were 19, 16 and 26 years of age, but, at the time of tumor diagnosis, all patients were under 19 years of age with presumed pediatric biology of their tumors. Two of the three patients met feasibility for generating a specified CAR T cell product, with 1.95×10^9 truncated EGFR$^+$ (EGFRt$^+$) cells generated for S001 and 3.16×10^9 EGFRt$^+$ cells generated for S002 (Table 1). S003's initial product failed viability screening, and two additional manufacturing attempts were ultimately required to generate sufficient numbers of CAR T cells to complete a minimum of two courses.

Manufacturing and phenotype of patient-derived HER2CAR T cell products. The BrainChild-01 HER2CAR T cell product was manufactured under a process designed to yield balanced numbers of CD4$^+$ and CD8$^+$ lentivirally transduced T cells exhibiting limited terminal differentiation with enrichment for the CAR$^+$

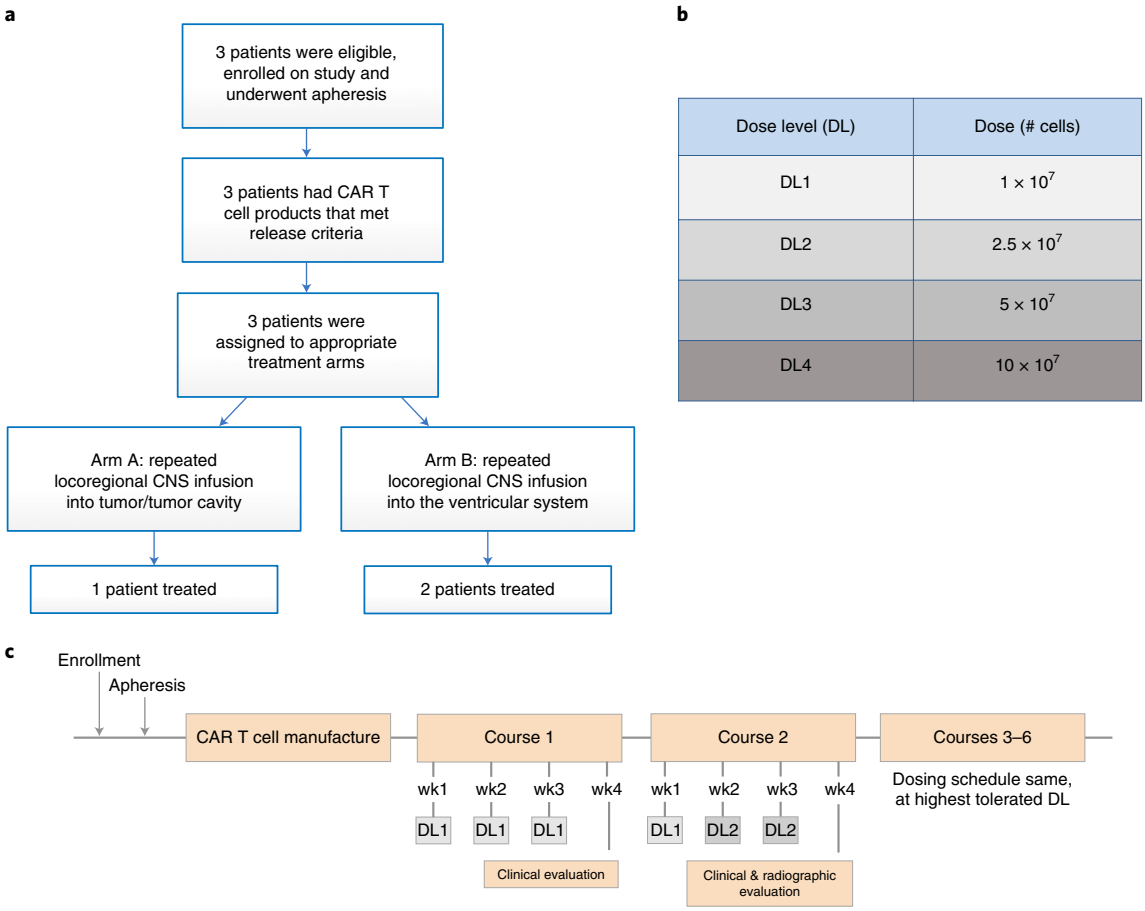

Fig. 1 | BrainChild-01 trial design. a, CONSORT diagram of BrainChild-01 interim analysis. Three patients were eligible and underwent apheresis, which led to a CAR T cell product meeting release criteria in all three patients. One patient was enrolled and treated on Arm A, and two patients were enrolled and treated on Arm B. **b**, Dose levels. **c**, Clinical trial schedule for patients enrolled on DR1. Patients undergo intra-patient dose escalation so, by completion of Course 2 (the end of the DLT window), patients have received four doses at DL1 and two doses at DL2. If study criteria are met, patients may elect to continue beyond Course 2 at DL2. Future patients enrolled on DR2 may dose escalate to DL3, and patients enrolled on DR3 may dose escalate to DL4. wk, week.

Table 1 | Patient demographics and CAR T cell product

	Arm[a]	Diagnosis	Sex	Age	Total nucleated cells manufactured	EGFRt$^+$ CAR T cells manufactured	Doses
S001	A	Anaplastic astrocytoma (WHO grade III), localized	F	19	1.95×10^9	1.87×10^9	6
S002	B	Ependymoma (WHO grade III), metastatic	M	16	3.2×10^9	2.97×10^9	9
S003	B	Ependymoma (WHO grade III), metastatic	M	26	2.06×10^{9b}	1.87×10^{9b}	9

[a]Arm A: localized disease with intra-tumoral CNS infusions; Arm B: metastatic disease with intra-ventricular CNS infusions. [b]Cumulative number from two CAR T cell products.

population of cells mid-culture (Extended Data Fig. 5 and Methods). The engraftment and therapeutic potency of cell products consisting of both CD4$^+$ and CD8$^+$ CAR T cells was previously described[22,28,29]. This manufacturing process targeted a 7-d expansion culture followed by EGFRt immunomagnetic selection to purify the product in favor of CAR T cells. After selection, cultures were continued to allow for recovery from the selection, and culture durations were based on in-process monitoring of viable cell numbers sufficient for patient dosing and, thus, were extended as needed. With an initial seed CD4$^+$:CD8$^+$ T cell ratio of 1:1, the final product CD4$^+$:CD8$^+$ T cell ratios were 47.8:55.8 (S001), 50.8:50.5 (S002), 65.8:28.1 (S003 (Final-02)) and 68.2:38.8 (S003 (Final-03)). The relationship between the input CD4$^+$:CD8$^+$ T cell ratio and that of the final product is best preserved over short culture durations, and the culture durations for S001, S002, S003 (Final-02) and S003 (Final-03) were 18 d, 14 d, 17 d and 15 d, respectively. These data support the balancing of input CD4$^+$ and CD8$^+$ T cells to generate balanced CD4$^+$:CD8$^+$ CAR T cell products.

We analyzed each patient's starting apheresis material and final CAR T cell products via multiparameter flow cytometry (Fig. 2a;

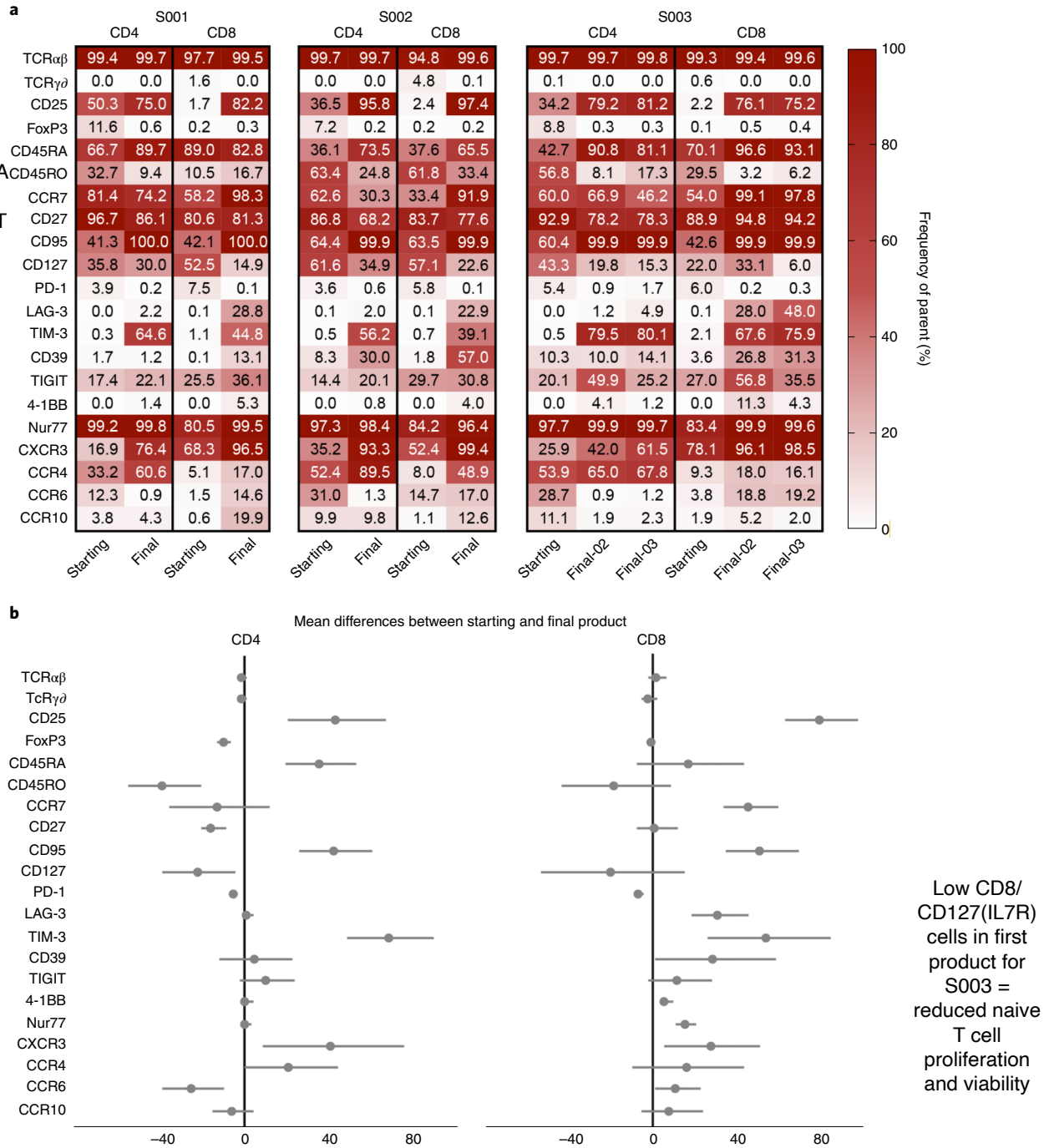

Retained high frequency of CD45RA and CD27, low CD45RO = no CAR T differentiation into terminal effectors

Low CD8/ CD127(IL7R) cells in first product for S003 = reduced naive T cell proliferation and viability

Fig. 2 | Defined input ratio of CD4⁺ and CD8⁺ T cells yields balanced CD4⁺CD8⁺ CAR T cell products. a, Comparison of the starting versus final product profile for the CD4⁺ and CD8⁺ T cell subsets for each patient (S001, S002 and S003; Final-02 and Final-03 refer to second and third manufacturing attempts for S003). Frequency of parent values are reported in each cell for the indicated marker. Representative flow gating strategy is shown in Supplementary Fig. 1. **b**, Mean (●) differences in marker expression between starting and final product. Horizontal bars show the 95% confidence interval for the mean difference. To account for S003 having two different products manufactured, estimates and confidence intervals were obtained using bootstrap resampling for clustered data.

representative flow gating strategy, Supplementary Fig. 1). Mean within-patient differences for each individual marker between CD4⁺ starting and final products or CD8⁺ starting and final T cell products are shown in Fig. 2b. CD8⁺ final T cell products retained high frequencies of CD45RA⁺ and CD27⁺ CAR T cells and a low frequency of CD45RO⁺ cells, demonstrating that ex vivo culturing did not differentiate CAR T cells to terminal effectors. The percentage of CD8⁺CCR7⁺ T cells in final products also increased markedly compared to starting CD8⁺ T cells (S001: 58.2–98.3%; S002: 33.4–91.9%; S003: 54.0–99.1% (Final-02) or 97.8% (Final-03)). Compared to S001 and S002, S003's initial CD8⁺ T cell population had a lower frequency of CD127 (IL-7R)-expressing cells. IL-7 promotes the homeostatic proliferation and survival of naive T cells, and lower CD127 expression is associated with more extensive

differentiation of their T cell repertoire[30–32] and an ensuing reduction in naive T cell proliferation and viability. Specifically, S003 had only 22.0% CD8$^+$CD127$^+$ starting T cells compared to 52.5% and 57.1% for S001 and S002, respectively.

We further compared marker co-expression profiles between starting and final products, specifically examining 4-1BB, LAG-3, PD-1 and TIGIT (Extended Data Fig. 6). CD8$^+$ T cell final products had increased LAG-3 and 4-1BB, and no PD-1 expression, compared to starting CD8$^+$ T cells. Products also had upregulated expression of CCR4, rendering them potentially sensitive to CCL2 chemokine, which is typically secreted by tumor cells and the tumor microenvironment stroma of brain tumors[33] (Fig. 2). Collectively, these data demonstrate the utility of our updated manufacturing process to generate CAR T cell products with balanced CD4$^+$ and CD8$^+$ T cell subsets.

Locoregional HER2-specific CAR T cells were well tolerated in the first three treated patients. CAR T cells are delivered weekly on Weeks 1, 2 and 3 of each 4-week course (Fig. 1c). Although the DLT window is two courses (that is, 2 months), if patients meet study criteria, they may elect to continue for a maximum of six courses (that is, 18 doses). In total, the three patients received 24 CAR T cell infusions, 12 at DL1 (1×10^7 cells) and 12 at DL2 (2.5×10^7 cells). S001 received a planned six infusions through Course 2, whereas S002 and S003 received Course 3 therapy for a total of nine locoregional infusions each. None of the patients experienced a DLT. The most consistent adverse events possibly, probably or definitely related to CAR T cell infusions were headache, pain (at metastatic sites of spinal cord disease) or transient worsening of a baseline neurologic deficit (Extended Data Figs. 7 and 8). Two patients (S002 and S003), both enrolled on Arm B with an intraventricular CNS catheter, also experienced fever within 24 h of their infusions. Elevation in systemic C-reactive protein (CRP) was observed in all patients, overlapping with timing of headache and/or pain.

As for any patient with a recurrent, malignant CNS tumor, quality of life (QOL) is strongly considered, and there is discussion with patients or their caretakers regarding palliative care consultation. Formal QOL findings are not reported here, as children enrolled on the BrainChild protocols enroll on institutional and national QOL studies, but, if possible, QOL will be reported at the completion of the trial.

CSF cytokines and radiographic imaging after HER2CAR T cell infusion. We sought to detect CAR T cells in CSF and peripheral blood from BrainChild-01 patients after infusion and analyze CSF and serum for potential biomarkers of anti-tumor CAR T cell activity. We did not detect CAR T cells in any patient at any time point after infusion in CSF (via flow cytometry; representative examples are shown in Extended Data Fig. 9, and representative gating strategy is shown in Supplementary Fig. 1) or in peripheral blood (via qPCR for CAR T cell DNA; no copy numbers were observed above the limit of detection—Supplementary Fig. 2). However, we did detect non-CAR T cell populations (both CD4$^+$ and CD8$^+$ T cells) in CSF after infusion.

We next measured cytokine/chemokine levels in CSF (Fig. 3a) and serum (Fig. 3b) from patients at various time points throughout their CAR T cell infusion schedule. After the initial infusion, patients had detectable levels of the following cytokines in the CSF: CXCL10, CCL2, G-CSF, GM-CSF, IFNα2, IL-10, IL12-p70, IL-15, IL-1α, IL-6, IL-7 and TNFα. Compared to pre-infusion, S002 and S003 exhibited elevated IFNγ, IL12-p40 and IL-3, and S003 had elevated VEGF (Fig. 3a). Strikingly, CXCL10, a type 1 CXC chemokine ligand, the synthesis of which is induced in a variety of cell types by IFNγ[34], was the most elevated chemokine detected, measured by absolute change, after initial infusion in CSF in patients S002 and S003 compared to their pre-infusion time point (S002: maximum concentration of CXCL10, 25,865 pg ml^{-1}; S003: maximum concentration of CXCL10, 19,543 pg ml^{-1}; Fig. 3a). CXCL10 was also the most elevated chemokine detected in S001 after initial CAR T cell infusion (S001: maximum concentration of CXCL10, 2,537 pg ml^{-1}), although no pre-infusion comparison was possible for this patient. Another chemokine detected at high concentrations after infusion was CCL2 (monocyte chemoattractant protein-1), which is produced by the tumor microenvironment and is critical for chemotaxis of regulatory T cells and myeloid-derived suppressor cells[35]. CCL2 in the CSF of patient S003 increased sharply after Course 1 Week 1 compared to pre-infusion and then remained relatively steady throughout subsequent infusions. In contrast, CCL2 was consistently high in S002 before infusion and throughout the infusion regimen (baseline level of CCL2 at pre-Course 1 Week 1 was higher than in S003). Compared to other measured cytokines, CCL2 and CXCL10 had the highest detectable concentrations in serum across all time points in all three patients (Fig. 3a). Serum cytokine levels also appeared relatively stable in all three patients across all CAR T cell infusions, with fewer fluctuations compared to CSF.

To further examine inflammatory responses in patients treated on BrainChild-01, we plotted CRP in serum alongside CXCL10 and CCL2 in CSF (Fig. 4). Patients exhibited transient serum CRP elevations after some CAR T cell infusions (S001: peak of 3.9 mg dl^{-1} after Course 1 Week 1 (although no pre-infusion comparison was possible for this patient); S002: peak of 2.3 mg dl^{-1} after Course 2 Week 1; and S003: peak of 1.7 mg dl^{-1} before Course 1 Week 2). High serum CRP for S001 (after Course 1 Week 1) and S002 (after Course 2 Week 1) correlated with maximum detection of CXCL10 in CSF. Additionally, for S001, CRP detection after Course 1 Week 1 and at Course 2 Week 4 corresponded with elevated CCL2 in CSF. For S003, serum CRP increased sharply after Course 1 Week 1 and before Week 2 infusion, which corresponded to a high concentration of CXCL10 detected in CSF. When presence of fever, presence of headache and neurotoxicity grade were overlayed, clinical symptoms showed a correlation with high concentrations of CXCL10 and CCL2 in CSF as well as serum CRP (Fig. 4). Taken together, these data demonstrate that all three patients exhibited local CNS inflammatory responses after CAR T cell infusion, with several cytokines detected in CSF and serum, particularly CXCL10 and CCL2.

Patients had neuroimaging performed at the end of Course 2 as per the protocol's scheduled observations, and one patient continues to have interval imaging performed 342 d after initial infusion. S001, who had localized disease, had transient increase of multiple baseline neurologic findings within 24 h of their first dose. As this was our first patient and their initial dose, we performed magnetic resonance imaging (MRI) to ensure that there were no acute intracranial events (Fig. 5). Although there were no acute findings of hemorrhage or impending herniation, when comparing an MRI 12 d before CAR T cell infusion (Figs. 5a–c) to 4 d after initial CAR T cell infusion (Fig. 5d–f), there was a substantial increase in peritumoral vasogenic edema, local mass effect and intensified contrast enhancement consistent with an inflammatory response. At completion of Course 2, S001 and S003 had progressive disease, whereas S002 had stable disease. This imaging temporally correlated with detection of inflammatory cytokines in CSF and serum CRP, suggesting local immune activation. Although a similar imaging time point was not available for S002 and S003, we also include more complete neuro-imaging of S001, S002 and S003, including S001's most recent MRI 152 d from their initial infusion and imaging after Course 3 for S002 and S003 (Fig. 5g–o).

Discussion

We present the preclinical development of HER2-specific CAR T cells against pediatric CNS tumors and show early clinical tolerability and correlative findings of CAR T cell-mediated local

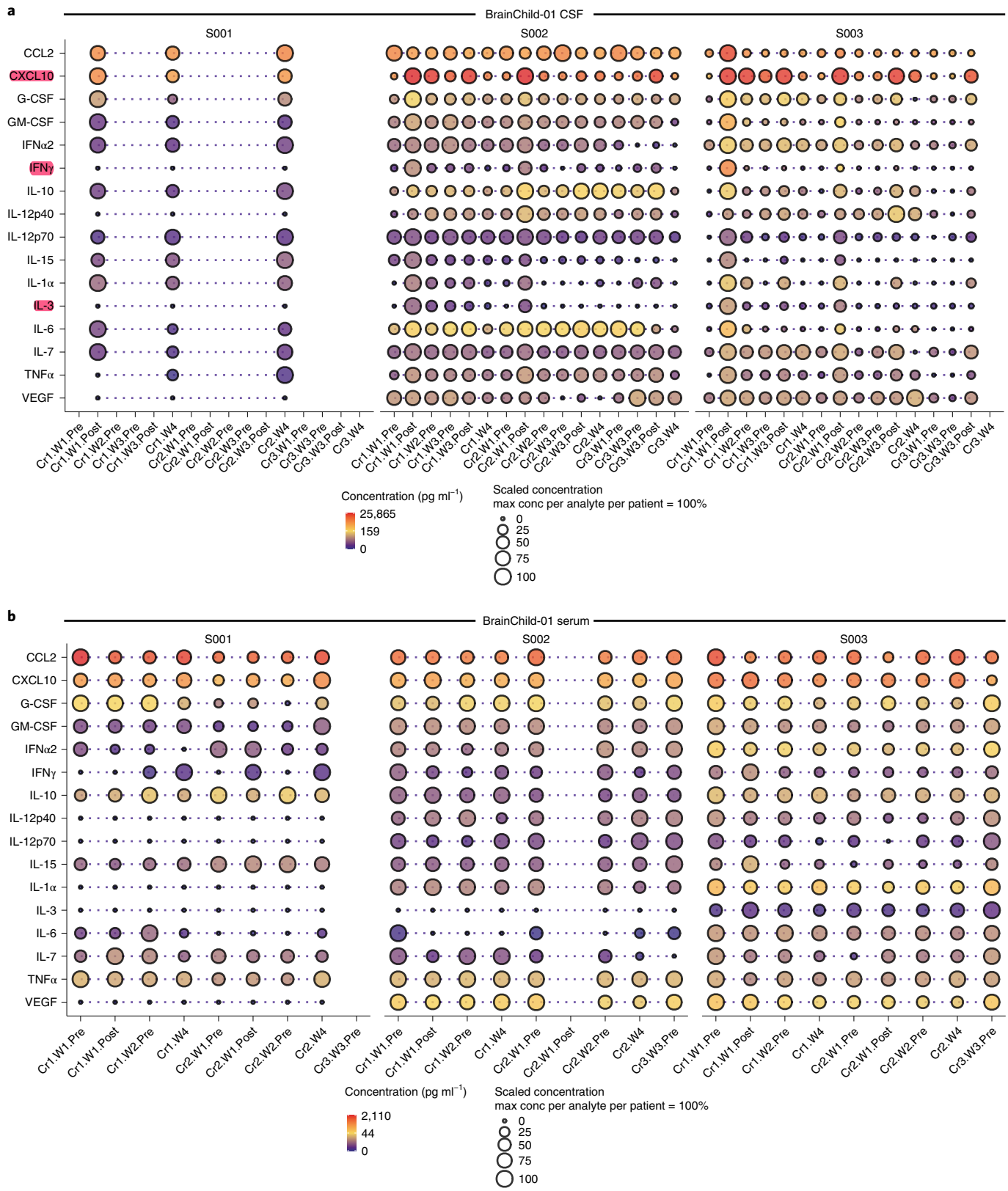

Fig. 3 | High concentrations of CXCL10 and CCL2 are detected after treatment in CSF samples. Cytokine concentrations in CSF (**a**) and serum (**b**) across all three patients were converted to $\log_2$ scale and represented with circles filled with color. Red color corresponds to the highest $\log_2$ concentration measured across all three patients for a given specimen type. Yellow and blue colors correspond to 50% and 0% of the $\log_2$ concentration, respectively. Additionally, concentrations relative to the maximum concentration observed for a given patient, specimen type and analyte are represented by the size of the circles, to highlight the fluctuation in cytokine concentrations throughout a patient's CAR T cell treatment. Cr, course; max conc, maximum concentration; W, week.

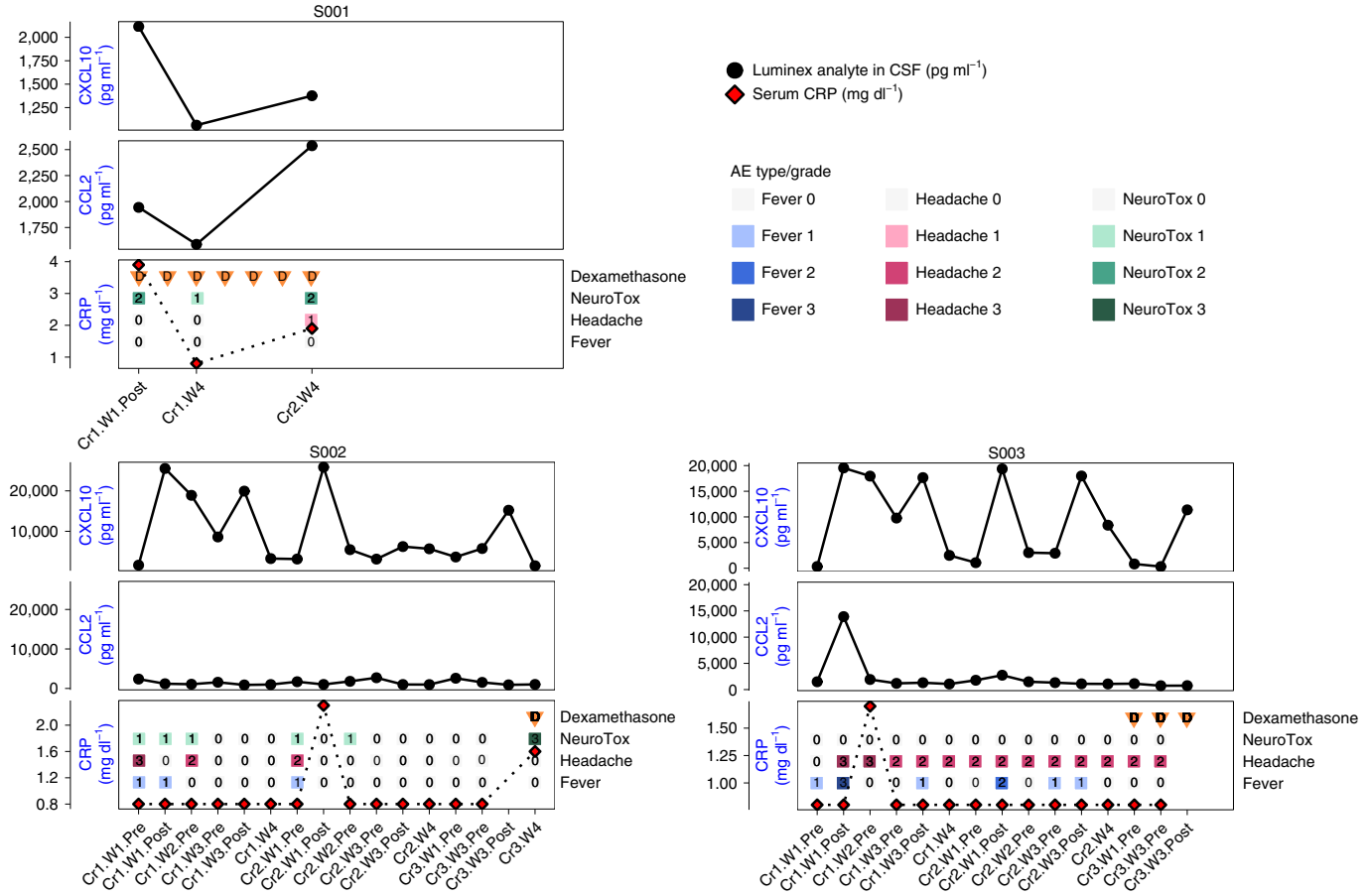

Fig. 4 | High concentrations of CXCL10 and CCL2 detected in CSF correlate with transient elevations in serum CRP. Serum CRP concentrations (in mg dl^{-1}) measured in clinical chemistry laboratory tests were plotted alongside CSF CXCL10 and CCL2 concentrations (in pg ml^{-1}) and clinical data (fever, headache and neurotoxicity) to illustrate trends throughout treatment courses for all three patients. S001 was on long-standing dexamethasone before enrollment and continued on dexamethasone throughout the study. S002 and S003 received dexamethasone only at time points (orange triangle D) marked in the figure. CAR T cell infusions were delivered between pre- and post-infusion time points during Weeks (W) 1, 2 and 3 of each course (Cr). For pre-infusion time points, correlative samples were taken before CAR T cell infusion; plotted adverse clinical events occurred on the same day but might have occurred after CAR T cell infusion (for example, fever in S002 and S003 at Cr1.W1.Pre). AE, adverse event; NeuroTox, neurotoxicity.

inflammation after intra-CNS delivery in patients with these tumors. Guided by preclinical data demonstrating the superiority of an M-spacer length HER2CAR, we initiated a phase 1 clinical trial delivering HER2-specific CAR T cells of a balanced CD4$^+$:CD8$^+$ ratio for children and young adults with HER2$^+$ CNS tumors. We observed symptoms consistent with on-target reactivity, without DLT, in the initial cohort of three patients. Although other groups have studied genetically modified cellular products targeting HER2 (refs. [4,5,36]), we delivered repetitive intracranial doses as a strategy to fractionate dosing for improved safety over a single large cell dose bolus and as a strategy to replenish local bioactive CAR T cells. In addition, we show correlative cytokine data consistent with pro-inflammatory immune cell activity in the CSF, potentially driven by CAR T cells in the tumor microenvironment. Neuroimaging in one of our patients shortly after their initial T cell infusion also demonstrated intra- and peri-tumoral changes consistent with acute local inflammation.

In our initial cohort of three patients, we were able to manufacture HER2-specific CAR T cell products in a predicted time frame for two of the three patients. S003 required additional CAR T cell manufacturing attempts to meet adequate product release criteria, which might have been related to a lower percentage of CD8$^+$ T cells expressing CD127 (IL-7R) in their starting material, as compared to S001 and S002. Final products across all three patients exhibited high percentages of cells expressing CD45RA, CCR7 or CD95 and low percentages of cells expressing CD45RO and FOXP3, consistent with phenotypic markers associated with retained engraftment fitness, as intended for an infused product[37].

HER2-specific CAR T cells and CAR T cell DNA, as measured in CSF and peripheral blood, respectively, were not detected after infusion in our patients. It is unclear if this was because of rapid demise of the cells, dispersion of the cells throughout the CSF, entry of the cells into the tumor or CNS interstitium or technical limitations in detection. We did, however, observe increases in non-CAR T cell populations in the CSF after CAR T cell infusion in two patients, suggesting the ability of CAR T cells, either by direct means or induced changes in the microenvironment, to influence other immune cells to enter the CNS or partition to the CSF compartment. It is also possible that endogenous T cells might traffic from the periphery, or that we are detecting expansion of a small proportion of CAR$^-$ cells in the infused product[38,39]. In the future, we will use T cell receptor (TCR) spectratyping to assess the composition of TCRs in cells in the CSF to determine overlap with the composition of TCRs expressed by cells in the infused product.

Notably, patients had high concentrations of CXCL10 and CCL2 in their CSF after treatment, which might provide a correlative readout of CAR T cell activity in situ. CXCL10 is upregulated by many cell types in response to IFNγ and promotes recruitment of

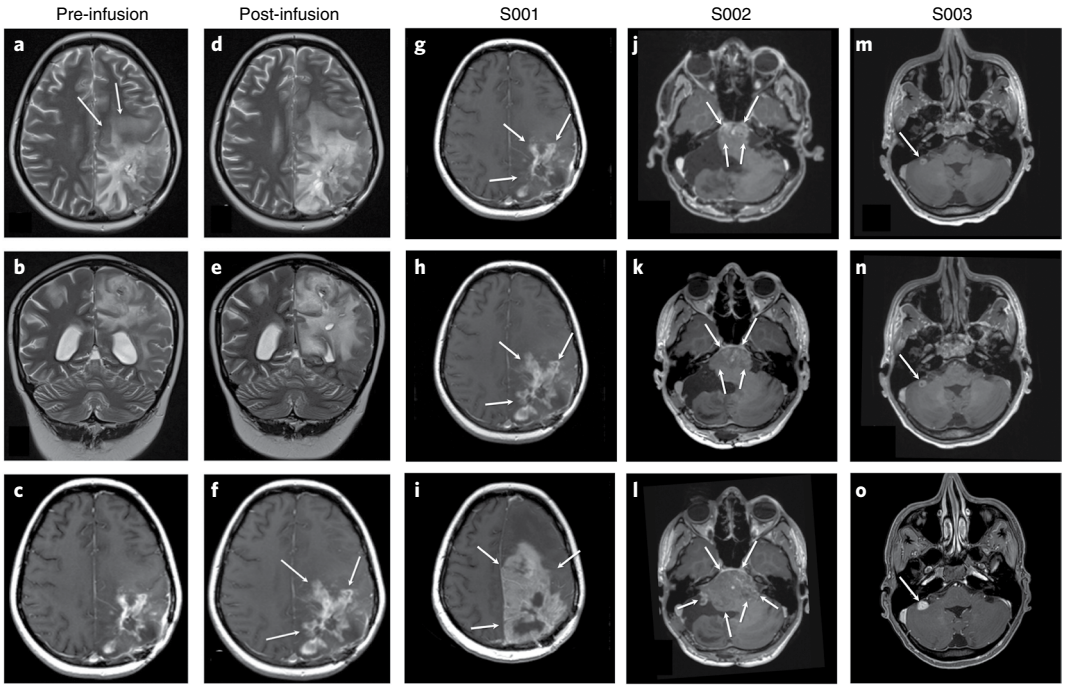

Fig. 5 | Neuro-imaging after locoregional CAR T cell infusion. Axial T2-weighted (**a**,**d**), coronal T2-weighted (**b**,**e**) and axial gadolinium-enhanced T1-weighted (**c**,**f**) images of S001 obtained 12 d before (**a**–**c**) and 4 d after (**d**–**f**) the first dose of CAR T cells. Images demonstrated a substantial increase in peritumoral vasogenic edema (white arrows), local mass effect (note new ventricular effacement between **b** and **e**) and contrast enhancement (white arrows) after CAR T cell administration, consistent with an inflammatory response. Axial contrast-enhanced T1-weighted images from all three patients immediately before initial CAR T cell administration (**g**,**j**,**m**), at first examination after CAR T infusion (**h**,**k**,**n**) and at the most recent available examination after CAR T cells but before any other tumor-directed therapy (**i**,**l**,**o**). Images correspond to study participants S001 (**g**,**h**,**i**; imaged at days −12, 4 and and 152 relative to first infusion); S002 (**j**,**k**,**l**; imaged at days −5, 49 and 90 relative to first infusion) and S003 (**m**,**n**,**o**; imaged at days −1, 15 and 81 relative to first infusion).

activated CXCR3$^+$ T cells to sites of inflammation and extravasation into tissue[40]. CD8$^+$ T cells require CXCL10 to traffic to gliomas[41–43], and CCL2 secretion by glioma tumor cells and tumor-associated macrophages directly mediates the homing of adoptively transferred CAR T cells to CNS tumors[33]. In our study, every patient's final CAR T cell product had higher frequencies of CXCR3$^+$ and CCR4$^+$ CAR T cells in both the CD4$^+$ T cell and CD8$^+$ T cell populations compared to their starting apheresis material. Final CAR T cell products with CXCR3 and CCR4 expression might be capable of chemotaxis to sites of CXCL10 and CCL2 expression, providing the potential for direct on-tumor, on-target engagement of CAR T cells that drives a localized immune response.

Our preclinical work was focused on medulloblastoma, so we cannot be certain that M-spacer HER2CAR T cells will have the highest activity against all pediatric CNS tumors, compared to T cells with CARs of other spacer lengths. Although the surfacesome differences among pediatric CNS tumors have not been as well characterized as the genomic landscape, particular surface antigen targets might be more relevant for specific subgroups, even within a defined pathologic group such as medulloblastoma. We note that, at the time of treatment, two of our first three patients were young adults, although their tumors are biologically pediatric CNS tumors, and they were children at the time of their cancer diagnosis. We expect the median age of treated patients will lower by study completion, as the initial three patients were required to be 15–26 years old, which is substantially higher than the median age of children with CNS tumors.

The clinical benefit of CAR T cell therapy might ultimately be dependent on target antigen density of the tumor; therefore, analyses will be performed, when possible, that assess the relationship between target antigen density and clinical toxicity and response. Tumor heterogeneity will continue to be an obstacle with single-antigen targeted cellular therapies, so we devised two additional locoregional CAR T cell clinical trials: BrainChild-02 (NCT03638167), delivering EGFR-specific CAR T cells to children with recurrent/refractory EGFR$^+$ CNS tumors, and BrainChild-03 (NCT04185038), delivering B7-H3-specific CAR T cells to children with recurrent/refractory CNS tumors as well as with diffuse intrinsic pontine glioma (DIPG). In our next CNS CAR T cell trial, we will build off the experiences of the BrainChild-01, BrainChild-02 and BrainChild-03 trials and use a multiplexed strategy to overcome tumor heterogeneity and antigen escape. Ultimately, the experience of the initial three patients treated on BrainChild-01 suggests that repeated locoregional HER2-specific CAR T cell dosing might be feasible and that correlative CSF markers might be valuable in assessing on-target CAR T cell activity in the CNS.

Online content

Any methods, additional references, Nature Research reporting summaries, source data, extended data, supplementary information, acknowledgements, peer review information; details of author contributions and competing interests; and statements of data and code availability are available at https://doi.org/10.1038/s41591-021-01404-8.

Received: 22 December 2020; Accepted: 25 May 2021;
Published online: 12 July 2021

References

1. Gardner, R. A. et al. Intent-to-treat leukemia remission by CD19 CAR T cells of defined formulation and dose in children and young adults. *Blood* **129**, 3322–3331 (2017).

2. Hudziak, R. M., Schlessinger, J. & Ullrich, A. Increased expression of the putative growth factor receptor p185HER2 causes transformation and tumorigenesis of NIH 3T3 cells. *Proc. Natl Acad. Sci. USA* **84**, 7159–7163 (1987).
3. Shen, L. et al. The efficacy of third generation anti-HER2 chimeric antigen receptor T cells in combination with PD1 blockade against malignant glioblastoma cells. *Oncol. Rep.* **42**, 1549–1557 (2019).
4. Ahmed, N. et al. HER2-specific chimeric antigen receptor-modified virus-specific T cells for progressive glioblastoma: a phase 1 dose-escalation trial. *JAMA Oncol.* **3**, 1094–1101 (2017).
5. Ahmed, N. et al. Regression of experimental medulloblastoma following transfer of HER2-specific T cells. *Cancer Res.* **67**, 5957–5964 (2007).
6. Choi, B. D., Curry, W. T., Carter, B. S. & Maus, M. V. Chimeric antigen receptor T-cell immunotherapy for glioblastoma: practical insights for neurosurgeons. *Neurosurg. Focus* **44**, E13 (2018).
7. Gilbertson, R. J., Pearson, A. D., Perry, R. H., Jaros, E. & Kelly, P. J. Prognostic significance of the c-*erb*B-2 oncogene product in childhood medulloblastoma. *Br. J. Cancer* **71**, 473–477 (1995).
8. Mineo, J. F. et al. Low HER2-expressing glioblastomas are more often secondary to anaplastic transformation of low-grade glioma. *J. Neuro-Oncol.* **85**, 281–287 (2007).
9. Cameron, D. et al. 11 years' follow-up of trastuzumab after adjuvant chemotherapy in HER2-positive early breast cancer: final analysis of the HERceptin Adjuvant (HERA) trial. *Lancet* **389**, 1195–1205 (2017).
10. Pegram, M. D. & Slamon, D. J. Combination therapy with trastuzumab (Herceptin) and cisplatin for chemoresistant metastatic breast cancer: evidence for receptor-enhanced chemosensitivity. *Semin. Oncol.* **26**, 89–95 (1999).
11. Slamon, D. J. et al. Use of chemotherapy plus a monoclonal antibody against HER2 for metastatic breast cancer that overexpresses HER2. *N. Engl. J. Med.* **344**, 783–792 (2001).
12. Pienkowski, T. & Zielinski, C. C. Trastuzumab treatment in patients with breast cancer and metastatic CNS disease. *Ann. Oncol.* **21**, 917–924 (2010).
13. Akhavan, D. et al. CAR T cells for brain tumors: lessons learned and road ahead. *Immunol. Rev.* **290**, 60–84 (2019).
14. Brown, C. E. et al. Regression of glioblastoma after chimeric antigen receptor T-cell therapy. *N. Engl. J. Med.* **375**, 2561–2569 (2016).
15. Brown, C. E. et al. Bioactivity and safety of IL13Rα2-redirected chimeric antigen receptor $CD8^+$ T cells in patients with recurrent glioblastoma. *Clin. Cancer Res.* **21**, 4062–4072 (2015).
16. Hudecek, M. et al. The nonsignaling extracellular spacer domain of chimeric antigen receptors is decisive for in vivo antitumor activity. *Cancer Immunol. Res* **3**, 125–135 (2015).
17. Wilkins, O., Keeler, A. M. & Flotte, T. R. CAR T-cell therapy: progress and prospects. *Hum. Gene Ther. Methods* **28**, 61–66 (2017).
18. Zhang, Z. et al. Modified CAR T cells targeting membrane-proximal epitope of mesothelin enhances the antitumor function against large solid tumor. *Cell Death Dis.* **10**, 476 (2019).
19. Haso, W. et al. Anti-CD22-chimeric antigen receptors targeting B-cell precursor acute lymphoblastic leukemia. *Blood* **121**, 1165–1174 (2013).
20. Brown, C. E. et al. Optimization of IL13Rα2-targeted chimeric antigen receptor T cells for improved anti-tumor efficacy against glioblastoma. *Mol. Ther.* **26**, 31–44 (2018).
21. Ravanpay, A. C. et al. EGFR806-CAR T cells selectively target a tumor-restricted EGFR epitope in glioblastoma. *Oncotarget* **10**, 7080–7095 (2019).
22. Shah, N. N. et al. CD4/CD8 T-cell selection affects chimeric antigen receptor (CAR) T-cell potency and toxicity: updated results from a phase I anti-CD22 CAR T-cell trial. *J. Clin. Oncol.* **38**, 1938–1950 (2020).
23. Andersch, L. et al. CD171- and GD2-specific CAR-T cells potently target retinoblastoma cells in preclinical in vitro testing. *BMC Cancer* **19**, 895 (2019).
24. Hudecek, M. et al. Receptor affinity and extracellular domain modifications affect tumor recognition by ROR1-specific chimeric antigen receptor T cells. *Clin. Cancer Res.* **19**, 3153–3164 (2013).
25. Guedan, S., Calderon, H., Posey, A. D. Jr. & Maus, M. V. Engineering and design of chimeric antigen receptors. *Mol. Ther. Methods Clin. Dev.* **12**, 145–156 (2019).
26. Donovan, L. K. et al. Locoregional delivery of CAR T cells to the cerebrospinal fluid for treatment of metastatic medulloblastoma and ependymoma. *Nat. Med.* **26**, 720–731 (2020).
27. Theruvath, J. et al. Locoregionally administered B7-H3-targeted CAR T cells for treatment of atypical teratoid/rhabdoid tumors. *Nat. Med.* **26**, 712–719 (2020).
28. Turtle, C. J. et al. CD19 CAR-T cells of defined $CD4^+$:$CD8^+$ composition in adult B cell ALL patients. *J. Clin. Invest.* **126**, 2123–2138 (2016).
29. Blaeschke, F. et al. Induction of a central memory and stem cell memory phenotype in functionally active $CD4^+$ and $CD8^+$ CAR T cells produced in an automated good manufacturing practice system for the treatment of $CD19^+$ acute lymphoblastic leukemia. *Cancer Immunol. Immunother.* **67**, 1053–1066 (2018).
30. Huang, W. & August, A. The signaling symphony: T cell receptor tunes cytokine-mediated T cell differentiation. *J. Leukoc. Biol.* **97**, 477–485 (2015).
31. Paiardini, M. et al. Loss of CD127 expression defines an expansion of effector $CD8^+$ T cells in HIV-infected individuals. *J. Immunol.* **174**, 2900–2909 (2005).
32. Gong, Y., Suzuki, T., Kozono, H., Kubo, M. & Nakano, N. Tumor-infiltrating $CD62L^+PD\text{-}1^-CD8$ T cells retain proliferative potential via Bcl6 expression and replenish effector T cells within the tumor. *PLoS ONE* **15**, e0237646 (2020).
33. Brown, C. E. et al. Tumor-derived chemokine MCP-1/CCL2 is sufficient for mediating tumor tropism of adoptively transferred T cells. *J. Immunol.* **179**, 3332–3341 (2007).
34. Okada, H. Brain tumor immunotherapy with type-1 polarizing strategies. *Ann. N. Y. Acad. Sci.* **1174**, 18–23 (2009).
35. Chang, A. L. et al. CCL2 produced by the glioma microenvironment is essential for the recruitment of regulatory T cells and myeloid-derived suppressor cells. *Cancer Res.* **76**, 5671–5682 (2016).
36. Zhang, C. et al. ErbB2/HER2-specific NK cells for targeted therapy of glioblastoma. *J. Natl Cancer Inst.* https://doi.org/10.1093/jnci/djv375 (2016).
37. Devaud, C., Darcy, P. K. & Kershaw, M. H. Foxp3 expression in T regulatory cells and other cell lineages. *Cancer Immunol. Immunother.* **63**, 869–876 (2014).
38. Li, X., Daniyan, A.F., Lopez, A.V., Purdon, T.J. & Brentjens, R.J. Cytokine IL-36γ improves CAR T-cell functionality and induces endogenous antitumor response. *Leukemia* **35**, 506–521 (2021).
39. Kuhn, N. F. et al. $CD103^+$ cDC1 and endogenous $CD8^+$ T cells are necessary for improved CD40L-overexpressing CAR T cell antitumor function. *Nat. Commun.* **11**, 6171 (2020).
40. Karin, N. CXCR3 ligands in cancer and autoimmunity, chemoattraction of effector T cells, and beyond. *Front. Immunol.* **11**, 976 (2020).
41. Fujita, M. et al. Effective immunotherapy against murine gliomas using type 1 polarizing dendritic cells—significant roles of CXCL10. *Cancer Res.* **69**, 1587–1595 (2009).
42. Nishimura, F. et al. Adoptive transfer of type 1 CTL mediates effective anti-central nervous system tumor response: critical roles of IFN-inducible protein-10. *Cancer Res.* **66**, 4478–4487 (2006).
43. Zhu, X. et al. Poly-ICLC promotes the infiltration of effector T cells into intracranial gliomas via induction of CXCL10 in IFN-α and IFN-γ dependent manners. *Cancer Immunol. Immunother.* **59**, 1401–1409 (2010).

Methods

Design of DNA constructs and lentivirus. The trastuzumab-based anti-HER2 scFv was assembled as previously described[44]. Variable short (IgG4-hinge), medium (IgG4-hinge-CH3) and long (IgG4-hinge-CH2-CH3) spacer second-generation 41BB-CD3ζ CARs were constructed using the V_L and V_H segments of trastuzumab, similarly to previously described CAR T cells[24,45]. An Lmut-spacer HER2CAR was created by mutating two key residues (L235D and N297Q) in the CH2 domain of the L-spacer HER2CAR to identify whether these CH2 modifications could rescue L-spacer in vivo activity, as previous CAR T cell studies have shown that wild-type IgG4-derived long spacers mitigate in vivo function[16]. Each CAR sequence was appended to a T2A ribosomal skip sequence followed by an EGFRt cell surface tag to facilitate selection[46]. Lentivirus was produced in HEK 293T cells using the packaging vectors pCHGP-2, pCMV-Rev2 and pCMV-G[24,25,47]. CAR expression levels were confirmed by scFv protein L staining and western blot for CD3ζ (Extended Data Fig. 1b,c; full western blot in Supplementary Fig. 3). Western blot analysis was performed using Image Studio software (LI-COR) version 3.1.

Production of CD8⁺ T cell lines expressing HER2CARs for preclinical analyses. CD8⁺ bulk T cells were isolated from peripheral blood mononuclear cells (PBMCs) of healthy donors (Bloodworks Northwest) by positive selection using CD8 microbeads (Miltenyi Biotec). After isolation, T cells were stimulated with anti-CD3/CD28 Dynabeads (Life Technologies) and transduced at a multiplicity of infection of 3 on the third day of culture. EGFRt⁺ T cell subsets were enriched by immunomagnetic selection using biotinylated cetuximab and anti-biotin microbeads (Miltenyi Biotec) and then expanded as previously described[21,23]. CD8⁺ T cells were maintained in RPMI medium (Gibco) supplemented with 10% FBS, 2 mM L-glutamine, 50 IU ml^{-1} of recombinant human IL-2 and 1 ng ml^{-1} of recombinant human IL-15.

Preclinical flow cytometry and immunophenotyping. Conjugated monoclonal antibodies for CD3, CD4, CD8, CD45RO and CD62L (BioLegend, 1:100 dilution) were used to immunophenotype various parental and enriched cell populations. Tumor cell HER2 positivity and CAR construct expression, via the surrogate cell surface marker EGFRt, were confirmed using biotinylated trastuzumab or cetuximab (1:1,000 dilution), respectively, and phycoerythrin (PE) conjugated streptavidin (SA-PE; BioLegend, 1:500 dilution). CAR cell surface and total expression was confirmed using biotinylated protein L (GenScript) and SA-PE or anti-CD247 (CD3ζ; BD Biosciences, 1:500 dilution), respectively. Spacer Fcγ receptor interactions were analyzed using biotinylated human and mouse FcγRI (Sino Biological, 1:100 dilution) and SA-PE. Flow analysis was performed on an LSRFortessa (BD Biosciences); sort purifications were performed on an FACSAria II (BD Biosciences); and data were analyzed using FlowJo software (BD Biosciences).

Cell line derivation and analysis. The D283 Med (ATCC HTB-185), D341 Med (ATCC HTB-187) and HEK 293T (ATCC CRL-3216) cell lines were obtained from the American Type Culture Collection (ATCC). These cell lines were maintained in DMEM (Gibco) supplemented with 2 mM L-glutamine (Irvine Scientific), 25 mM HEPES (Irvine Scientific) and 10% heat-inactivated FCS (HyClone). The patient-derived medulloblastoma cell culture Med411FH was generously provided by J. Olson (Fred Hutchinson Cancer Research Center). Med411FH cells were cultured in DMEM/F12 (Gibco) supplemented with B27, 15 mM HEPES, 2 mM L-glutamine, heparin and 20 ng ml^{-1} of rhEGF and rhFGF. Epstein–Barr virus-transformed lymphoblastoid cells lines (TM-LCLs) were made from PBMCs, as previously described, and were maintained in RPMI medium (Gibco) supplemented with 10% FBS and 2 mM L-glutamine[48]. All cell lines were authenticated by short tandem repeat profiling matched to the DSMZ (Deutsche Sammlung von Mikroorganismen und Zellkulturen) Database (University of Arizona Genetics Core). Total HER2 expression was analyzed by western blot analysis (Cell Signaling). LCL-HER2 and LCL-HER2t:CD19t were generated by lentiviral transduction (HER2t:CD19t contains an N-term GMCSFRss followed by aa 563–653 of HER2 and aa 20–323 of CD19) and enriched by immunomagnetic selection using biotinylated trastuzumab and anti-biotin microbeads (Miltenyi Biotec). D283 eGFP:ffluc tumor cells were generated by lentiviral transduction and sorted by FACSAria II (BD Biosciences).

Orthotopic xenograft model and exogenous T cell transplantation. Mutations (L235D and N297Q) to abrogate FcγR interactions were introduced into the CH2 region of the L-spacer CAR (designated Lmut spacer) before the onset of in vivo studies. The introduced mutations removed L-spacer human and mouse FcγR interactions and had no observed effect on CAR in vitro cytolytic activity (Supplementary Fig. 4). The orthotopic xenograft model was performed as previously described[21]. Briefly, 8–12-week-old adult male NOD/Scid IL-2RCnull (NSG) mice were injected intracranially on day 0 with 2×10^5 ffluc⁺IL2⁺ or eGFP:ffluc-expressing D283 tumor cells 2 mm lateral and 0.5 mm anterior to bregma and 2.5 mm and 2.25 mm deep from the dura. Mice were subsequently intracranially injected with a total of 2×10^6 CD8⁺ T cells 7 d later, 2.5 mm, 2.35 mm and 2.25 mm deep from the dura. The intracerebroventricular metastatic medulloblastoma xenograft model was similarly performed at coordinates 0.9 mm lateral and 0.3 mm caudal to bregma. Bioluminescent imaging was first performed on day 6 after tumor inoculation. Mice were distributed so that treatment groups had similar median bioluminescence and standard deviations. Bioluminescent imaging then was performed weekly by intraperitoneal injection of 4.29 mg per mouse of D-luciferin (Xenogen) after anesthetization by isoflurane. Imaging occurred 15 min after D-luciferin injection using the IVIS Spectrum Imaging System (PerkinElmer). Luciferase activity was analyzed using Living Image Software version 4.5.2 (PerkinElmer), and photon flux was analyzed within regions of interest. All animal experiments were approved by the Seattle Children's Research Institute Animal Care and Use Committee.

In vitro cellular assays. Purified (>95% EGFRt⁺) HER2CAR T cells were used for all in vitro assays. Chromium release assay: CD8⁺ T cell cytotoxicity was determined by chromium release assay. Target cells were labeled with Cr-51 (PerkinElmer), washed and incubated in triplicate with T cells at various effector-to-target ratios. Supernatants were harvested 4 h later for γ-counting using a TopCount NXT (software version 3.01) microplate scintillation and luminescence counter (PerkinElmer), and specific lysis was calculated using the standard formula[49]. Cytokine release assay: To investigate cytokine secretion, CD8⁺ T cells and target cells were plated at a 2:1 ratio, and supernatant was analyzed for IL-2, IFNγ and TNFα production after 24-h incubation using the Bio-Plex multiplex bead array system (Bio-Rad).

Preclinical statistical analyses. Statistical analyses were conducted using Prism software (GraphPad). Data are presented as mean ± s.d. or s.e.m., as stated in the figure legends. Student's *t*-test was conducted as a two-sided unpaired test with a confidence interval of 95%, and statistical analyses of survival were conducted by log-rank testing. Results with a *P* value less than 0.05 were considered significant.

Study design and participants. BrainChild-01 (NCT03500991) is a phase 1 study of CNS locoregional adoptive therapy with autologous CD4⁺ and CD8⁺ T cells lentivirally transduced to express a HER2-specific CAR and EGFRt, delivered by an indwelling catheter in the tumor resection cavity (Arm A) or the ventricular system (Arm B), in children and young adults with recurrent or refractory HER2⁺ CNS tumors, including diffuse midline glioma. This is a single-site clinical trial conducted at Seattle Children's Hospital. Accrual began on 15 June 2018. The first patient described in the manuscript, S001, enrolled on 26 July 2018, and the final patient described in the manuscript, S003, enrolled on 11 February 2020.

This study is conducted in accordance with the U.S. Food and Drug Administration (FDA) and International Conference on Harmonization Guidelines for Good Clinical Practice, the Declaration of Helsinki and applicable institutional review board requirements (study protocol approved by the Seattle Children's Institutional Review Board). All patients or their guardians provided written informed consent in accordance with local regulatory review. Enrollment criteria included: age ≥15 and ≤26 years for the initial three patients, followed by age criteria ≥1 and ≤26 years; histologically diagnosed HER2⁺ CNS tumor; evidence of refractory or recurrent CNS disease; ability to tolerate apheresis; presence of a CNS catheter; life expectancy of a minimum of 8 weeks; Lansky/Karnofsky performance score ≥60; defined washout periods from previous therapies; adequate organ function, including absolute lymphocyte count ≥500 cells per µl, absolute neutrophil count ≥500 cells per µl, hemoglobin ≥9 g dl^{-1}, platelets ≥100,000 per µl, creatinine less than or equal to the upper limit of normal (ULN) for age, bilirubin <3× ULN for age or conjugated bilirubin <2 mg dl^{-1}, oxygen saturation ≥93% without dyspnea at rest and adequate neurologic function, defined as stable deficits for ≥1 week, ≤2 anti-epileptic agents required to control seizures and no encephalopathy; negative virology for HIV, hepatitis B and hepatitis C; and use of highly effective contraception in patients of child-bearing age. HER2 positivity was determined by immunohistochemistry performed in an accredited facility with either an FDA-approved test or a test that meets accreditation standards. If performed at a referring hospital, Seattle Children's neuropathology confirmed HER2 positivity (defined as ≥2+ staining intensity in ≥10% of cells) before enrollment. Exclusion criteria included: diagnosis of DIPG; grade 3 or higher severe cardiac dysfunction or symptomatic arrythmia requiring intervention; primary immunodeficiency or bone marrow failure syndrome; clinical or radiographic evidence of impending CNS herniation; another active malignancy other than the CNS malignancy required for enrollment; active, severe infection defined as a positive blood culture within 48 h of enrollment or fever with clinical signs of infection; active receipt of any anti-cancer therapy; pregnancy or breastfeeding; patient and/or legal representative unwilling to provide consent/assent for study participation, including participation in the 15-year follow-up period required if CAR T cell therapy is administered; or the presence of any condition that, in the opinion of the investigator, would prohibit the patient from undergoing treatment under this protocol.

Patients were enrolled on either Arm A, using intra-tumoral CNS catheters, or Arm B, using intra-ventricular CNS catheters, dependent on disease location (Fig. 1a). Enrolled patients underwent leuko-pheresis. CD4⁺ and CD8⁺ T cells from apheresis products were bioengineered to express our HER2-targeting, second-generation CAR with an M-spacer length (Extended Data Fig. 1a). BrainChild-01 included intra-patient DL escalations over two 4-week courses

(Fig. 1b,c) with weekly CAR T cell dosing on Weeks 1, 2 and 3 of each 4-week course. Requirements to receive CAR T cell infusions included: evidence of persistence disease; ≥5 d from surgery; meeting defined washout periods from any bridging therapy; adequate organ function, defined by specified laboratory values used for eligibility; no encephalopathy or uncontrolled seizure activity; and compliance with prescribed anti-epileptic drug administration. To receive subsequent infusions, patients were also required to have had either no DLT if the previous infusion was at DL1 or resolution of any previous DLT to grade lower than 2 if the previous infusion was at DL2. Patients were eligible to receive additional infusions through Course 6 (maximum 18 doses) at the previous maximum tolerated dose level if above criteria were met and sufficient CAR T cells were available. Patients were enrolled into DRs with the potential for intra-patient dose escalation. In DR1, patients may escalate to DL2; in DR2, patients may escalate to DL3; and in DR3, patients may escalate to DL4. Response was assessed using CNS MRI after Courses 2, 4 and 6. Correlative studies collections varied by biospecimen and by assigned arm. For patients enrolled on Arm A, CSF for correlative studies was collected in Week 4 of Courses 1, 2, 4, 5 and 6. For patients enrolled on Arm B, CSF for correlative studies was collected in (1) Course 1 at Week 1 before and after infusion, Week 2 before infusion, Week 3 before and after infusion and Week 4; (2) Course 2 at Week 1 before and after infusion, Week 2 before infusion, Week 3 before and after infusion and Week 4; (3) Courses 3–6 at Week 1 before infusion, Week 3 before and after infusion and Week 4; and (4) at the end of therapy. All enrolled patients had peripheral blood for correlative studies collected at (1) Course 1 at Week 1 before and after infusion, Week 2 before infusion and Week 4; (2) Course 2 at Week 1 before and after infusion, Week 2 before infusion and Week 4; (3) Courses 3–6 at Week 3 before infusion; and (4) at the end of therapy.

Cell product manufacture. $CD4^+$ and $CD8^+$ T cells were isolated from patient apheresis products using the CliniMACS device (Miltenyi Biotec). A 1:1 mixture of CD4-enriched and CD8-enriched cell fractions was then pooled, suspended in X-VIVO 15 (Lonza) media supplemented with 2% KnockOut Serum Replacement (Life Technologies), 5 ng ml^{-1} of rhIL-7 (CellGenix), 0.5 ng ml^{-1} of rhIL-15 (CellGenix) and 10 ng ml^{-1} of rhIL-21 (Miltenyi Biotec), initiated into culture in a G-Rex 100MCS vessel (Wilson-Wolf) and stimulated using CD3/CD28 CTS Dynabeads (Life Technologies). Cell products were then transduced with a GMP-grade SIN (self-inactivating) lentivirus encoding the anti-HER2 CAR and the cell-surface marker EGFRt. On day 7 of culture, patient cell products were enriched for EGFRt-expressing cells using the CliniMACS device. After 14–18 d in culture, patient cells were harvested and washed using the Sepax 2RM device (GE) and resuspended in CryoStor CS5 (Biolife Solutions) for cryopreservation in CellSeal closed system vials (Sexton). The clinical culture conditions vary from the initial preclinical conditions, because, between initial preclinical investigations of our HER2CAR and the opening of BrainChild-01, the conditions considered to be optimal for our CAR T cell cultures evolved.

The process involved immunomagnetic positive selection of $CD4^+$ and $CD8^+$ T cells from the patients' apheresis products, followed by the seeding of cultures with defined input ratios of these cells, with the goal of having balanced ratios of $CD4^+$ and $CD8^+$ T cells at the end of a single-culture manufacturing procedure. In addition, homeostatic cytokines IL-7, IL-15 and IL-21 were supplemented into cultures, and exogenous IL-2 was not provided, to limit terminal differentiation and enrich for T cells expressing phenotypic markers associated with engraftment fitness. Lastly, cell products at the end of culture were purified for CAR expression by immunomagnetic positive selection of T cells expressing EGFRt, before cryopreservation.

Evaluations. The primary objectives of this study are to assess the feasibility, safety and tolerability of CNS locoregional adoptive therapy with autologous $CD4^+$ and $CD8^+$ T cells lentivirally transduced to express a HER2-specific CAR and EGFRt, delivered by an indwelling catheter in the tumor cavity or ventricular system, in children and young adults with recurrent/refractory $HER2^+$ CNS tumors. Feasibility is defined as generating sufficient therapeutic product to receive a minimum of six doses at the intended DL per assigned DR, after two attempts using a single apheresis product for starting material. Safety and tolerability are determined by data that include history/physical exams, laboratory/radiographic evaluations and Common Terminology Criteria for Adverse Events (CTCAE) version 5.0. A DLT is defined as an event that, in the opinion of the investigator, is possibly, probably or definitely attributable to the CAR T product and that occurs from the time of initial CAR T cell infusion through 28 d after the final CAR T cell infusion. A DLT includes all grade 3 or higher CTCAE v5.0 toxicities except grade 3 or higher toxicities that are known to be related to CAR T cells, including grade 4 CRS that decreases to grade 2 or lower within 72 h; grade 3 CRS that decreases to grade 2 or lower within 7 d; grade 3 or higher hypotension, fever and/or chills not controlled with medical intervention that decrease to grade 2 or lower within 72 h; grade 3 or higher activated prothrombin time, fibrinogen and/or international normalized ratio that are asymptomatic and resolve within 72 h; grade 3 or higher hypoglycemia and/or electrolyte imbalance that are asymptomatic and resolve within 72 h; grade 3 or higher nausea and/or vomiting that decrease to grade 2 or lower with 7 d; and grade 3 or higher neurologic symptoms that decrease to grade 2 or lower with 7 d. The definition of a DLT also includes any toxicity lasting more than 14 d that prevents the patient from meeting criteria for subsequent CAR T cell infusion. Secondary objectives of this study are to assess CAR T cell distribution within the CSF and the extent to which CAR T cells egress to the peripheral circulation, as measured by qPCR; to assess whether HER2 expression changes in relapsed CNS tumors that were $HER2^+$ before treatment with CAR T cells, as measured by immunohistochemistry; and to assess disease response to HER2-specific CAR T cell CNS-directed therapy, as measured by neuroimaging and clinical course.

Patients are assigned a neurotoxicity score at each clinical evaluation during protocol therapy. Toxicity grade ranges from 0 to 5: 0 is normal or no change from baseline examination at the start of therapy; 1 is mild lethargy and/or irritability or visual, motor or sensory symptoms without change in neurological exam; 2 is moderate lethargy, disorientation or psychosis lasting less than 48 h or mild increase in preexisting neurological deficit; 3 is more than 48 h of severe lethargy, responsiveness to verbal stimuli, disorientation or psychosis lasting more than 48 h, moderate increase in preexisting neurological deficit or the onset of new neurological signs or more than two seizures in 24 h; 4 is coma, unresponsive to verbal stimuli, increasing neurologic deficit higher than grade 3, evidence of herniation, development of uncontrolled seizures or intracerebral hemorrhage; 5 is death.

Flow cytometry of CAR T cell products and correlative specimens. Immunophenotyping of surface markers on starting and final products was performed using standard staining and flow cytometry techniques, with combinations of the following fluorophore-conjugated anti-human monoclonal antibodies: CD3 (BD Biosciences, cat. no. 562426, RRID:AB_11152082, 1.25 µl per test, or BD Biosciences, cat. no. 652356, RRID:AB_2868395), CD4 (BD Biosciences, cat. no. 562658, RRID:AB_2744420, 2.5 µl per test), CD8α (BD Biosciences, cat. no. 560662, RRID:AB_1727513, 0.63 µl per test), CD36 (BD Biosciences, cat. no. 555454, RRID: AB_2291112, 2.5 µl per test), CD25 (BD Biosciences, cat. no. 564034, RRID:AB_2738556, 0.31 µl per test), CD27 (BD Biosciences, cat. no. 564301, RRID:AB_2744350, 2.5 µl per test), CD39 (BioLegend, cat. no. 328212, RRID:AB_2099950, 1.25 µl per test), CD45RA (BD Biosciences, cat. no. 563870, RRID:AB_2738459, 2.5 µl per test), CD45RO (BD Biosciences, cat. no. 564291, RRID:AB_2744410, 1.25 µl per test), CD95 (BD Biosciences, cat. no. 561633, RRID:AB_10894384, 0.63 µl per test), CD127 (BD Biosciences, cat. no. 563324, RRID:AB_2738138, 1.25 µl per test), CD137 (BioLegend, cat. no. 309820, RRID:AB_2563830, 5.0 µl per test), CCR4 (BioLegend, cat. no. 359410, RRID:AB_2562431, 0.63 µl per test), CCR6 (BD Biosciences, cat. no. 563704, RRID:AB_2738381, 1.25 µl per test), CCR7 (BD Biosciences, cat. no. 552176, RRID:AB_394354, 1.25 µl per test), CCR10 (BD Biosciences, cat. no. 563656, RRID:AB_2738351, 0.63 µl per test), CXCR3 (BD Biosciences, cat. no. 565223, RRID:AB_2687488, 5.0 µl per test), FoxP3 (BD Biosciences, cat. no. 560045, RRID:AB_1645411, 10.0 µl per test), LAG-3 (BioLegend, cat. no. 369310, RRID:AB_2629753, 5.0 µl per test), Nur77 (Thermo Fisher Scientific, cat. no. 12-5965-82, RRID:AB_1257209, 2.5 µl per test), PD-1 (BD Biosciences, cat. no. 565299, RRID:AB_2739167, 2.5 µl per test), TCRαβ (BD Biosciences, cat. no. 564725, RRID:AB_2738918, 2.5 µl per test), TCRγδ (BD Biosciences, cat. no. 655434, RRID:AB_2827402, 2.5 µl per test), TIGIT (BioLegend, cat. no. 372712, RRID:AB_2632927, 1.25 µl per test) and TIM-3 (BioLegend, cat. no. 345032, RRID:AB_2565833, 2.5 µl per test). CAR T cell expression was quantified using cetuximab (Creative Diagnostics, cat. no. TAB-003, RRID:AB_2459632, 1:50 dilution) custom conjugated to allophycocyanin by BD Biosciences to detect EGFRt. Cells were also stained with a live/dead viability dye (BD Biosciences, cat. no. 564407, 1:16,000 dilution). Intracellular staining was performed according to manufacturer directions with the Transcription Factor Buffer Set (BD Pharmingen, cat. no. 562574) for FoxP3 detection or the Fixation/Permeabilization Solution Kit (BD Biosciences, cat. no. 554714) for Nur77 detection. Cells were acquired on an LSRFortessa (BD Biosciences), and flow cytometric analysis was performed using FlowJo software (BD Biosciences). CAR T cells were defined as a singlet, viable, $CD36^-$, $CD3^+$, $EGFR^+$, $CD4^+$ or $CD8^+$ lymphocytes. In general, markers of interest were examined in the $EGFRt^-$ or $EGFRt^+$ populations as applicable for starting or final product samples, with the exception of CD25, CD127, FoxP3, TCRαβ and TCRγδ. These markers were stained in a flow cytometry panel that did not include EGFRt selection and are, therefore, reported as a percentage of the total $CD4^+$ or $CD8^+$ T cell population. Multi-activation marker profiles were analyzed via Boolean gating and SPICE analysis software[50]. Representative flow gating is shown in Supplementary Fig. 1.

qPCR for CAR T cell persistence. Assessment of persistence of CAR T cells in peripheral blood was determined by quantification of the Flap-EF1 region of the lentiviral transgene by qPCR. Patient genomic DNA isolated from mononuclear cells from specific time points was assessed for in vivo persistence by batched analysis. Standard curve for the transcript copy number was established by the amplification of serial diluted plasmid epHIV7. The number of copies of the transgene per nanogram of genomic DNA input was determined.

Cytokine profiling. Patient CSF or serum samples were collected and processed by the study site before cryopreservation at −80 °C. CSF was collected by either

lumbar puncture or ventricular/cavity catheter and maintained at 4 °C before and during cell-free supernatant isolation by serial centrifugation. Cells were removed from the CSF sample by spinning at 250*g* for 10 min followed by a final debris removal spin at 10,000*g* for 10 min. Serum was isolated by collection of venous blood in additive-free collection tubes. After incubation at room temperature for a minimum of 1 h, collection tubes were centrifuged at 1,000*g* for 15 min. The resulting supernatant was subsequently centrifuged at 10,000*g* for 10 min before aliquoting and transfer to storage. Samples were thawed and assessed by batched analysis for select cytokines and chemokines according to manufacturer instructions for the 29-plex Human Cytokine/Chemokine Luminex kit (Millipore, cat. no. HCYTMAG60PMX29BK). The Millipore Human Cytokine/Chemokine Panel is a multiplex sandwich capture assay using magnetic antibody-coupled beads that bind cytokine molecules of interest in the CSF or serum sample, biotinylated detection antibody specific for a different epitope on the cytokine and secondary streptavidin-PE antibody to label the bead–cytokine complex. All samples and controls were run in duplicate. Samples were analyzed in a flow-based suspension system, and the cytokine concentrations in the samples were extrapolated from the general five-parameter standard curve using Millipore cytokine standard reagent. CXCL10 concentrations for Arm B patients (S002 and S003) at several time points were higher than the highest standard used in the experiment. Rather than use concentrations of the highest standards, we extrapolated concentrations from the five-parameter standard curve and used the extrapolated values in our analyses. Serum CRP concentrations were measured in clinical chemistry laboratory tests and were plotted alongside CXCL10 and CCL2 concentrations in CSF. Heat maps and line plots were generated using R (v3.6.3)[51] with ggplot2 library (v3.3.0)[52].

Correlative sample statistical analysis. Data on marker expression in the starting and final $CD4^+$ and $CD8^+$ T cell products were summarized. For each marker, the mean within-patient difference in expression between starting and final products is presented, along with a 95% confidence interval for the mean difference. Because one patient had two different products generated, estimates and confidence intervals were obtained using bootstrap resampling for clustered data. Bootstrap resampling (10,000 iterations) was done with Stata 16.1 (Stata Statistical Software: Release 16, StataCorp).

Statistical significance for pie charts was determined using the non-parametric partial permutation (Monte Carlo simulation) analysis in SPICE software, with 10,000 iterations per test.

Reporting Summary. Further information on research design is available in the Nature Research Reporting Summary linked to this article.

Data availability

All requests for raw and analyzed data and materials will be promptly reviewed by the intellectual property office of Seattle Children's Research Institute to verify if the request is subject to any intellectual property or confidentiality obligations. Raw preclinical and clinical data are stored at Seattle Children's with indefinite appropriate backup. The full raw western blot is shown in Supplementary Fig. 3. Patient-related data not included in the paper were generated as part of clinical trials and might be subject to patient confidentiality. Any data and materials that can be shared will be released via a material transfer agreement.

References

44. Zhao, Y. et al. A Herceptin-based chimeric antigen receptor with modified signaling domains leads to enhanced survival of transduced T lymphocytes and antitumor activity. *J. Immunol.* **183**, 5563–5574 (2009).
45. Kunkele, A. et al. Functional tuning of CARs reveals signaling threshold above which $CD8^+$ CTL antitumor potency is attenuated due to cell Fas–FasL-dependent AICD. *Cancer Immunol. Res.* **3**, 368–379 (2015).
46. Wang, X. et al. A transgene-encoded cell surface polypeptide for selection, in vivo tracking, and ablation of engineered cells. *Blood* **118**, 1255–1263 (2011).
47. Watanabe, N. et al. Fine-tuning the CAR spacer improves T-cell potency. *Oncoimmunology* **5**, e1253656 (2016).
48. Pelloquin, F., Lamelin, J. P. & Lenoir, G. M. Human B lymphocytes immortalization by Epstein–Barr virus in the presence of cyclosporin A. *Vitr. Cell Dev. Biol.* **22**, 689–694 (1986).
49. Erskine, C.L., Henle, A.M. & Knutson, K.L. Determining optimal cytotoxic activity of human Her2neu specific CD8 T cells by comparing the Cr51 release assay to the xCELLigence system. *J. Vis. Exp.* e3683 (2012).
50. Roederer, M., Nozzi, J. L. & Nason, M. C. SPICE: exploration and analysis of post-cytometric complex multivariate datasets. *Cytom. A* **79**, 167–174 (2011).
51. R Core team. R: A Language and Environment for Statistical Computing (R Foundation for Statistical Computing, 2014).
52. Wickham, H. *ggplot2: Elegant Graphics for Data Analysis* (Springer, 2016).

Acknowledgements

We thank the children and families who bravely shoulder the burden of their disease and place their trust in Seattle Children's. We are indebted to our clinical research team, including H. Ullom, A. Thomsen, V. Weiss, K. Cilluffo, E. Stowe and G. Mun. We are grateful for the clinical expertise of our neuro-oncology team, including R. Geyer, J. Olson, S. Leary, N. Millard, A. Sato, E. Crotty, C. Hoeppner, S. Holtzclaw, S. Chaffee, A. Laurine, S. Stasi, B. Cole, F. Perez, M. Susun and W. Iwata. We thank J. Stevens, as well as the Seattle Children's Hospital's Department of Anatomic Pathology and Seattle Children's Tumor Bank, for assistance in tissue collection and research coordination, and C. Schubert for editorial assistance. We thank the Therapeutic Cell Production Core for their tireless efforts to manufacture infusion products and the Correlative Studies Lab for their assistance in research coordination and correlative sample processing. Funding: We are grateful for generous funding from the Seattle Run of Hope (N.A.V.), the Pediatric Brain Tumor Research Fund Guild of Seattle Children's Hospital (N.A.V.), the McKenna Claire Foundation (N.A.V.), Unravel Pediatric Cancer (N.A.V.), Team Cozzi Foundation (N.A.V.), Love for Lucy (N.A.V.), the Julianna Sayler Foundation (N.A.V.), the Avery Huffman DIPG Foundation (N.A.V.), Liv Like a Unicorn (N.A.V.), ImmunoMomentum! (N.A.V., N.P., M.C.J.), Amazon (N.A.V., M.C.J.), the DIPG All-In Initiative (N.A.V.) and St. Baldrick's Stand Up to Cancer (SU2C) Dream Team Translational Cancer Research Grants (SU2C-AACR-DT-27-17 to N.A.V., R.J.O., R.G., M.C.J. and J.R.P.). Stand Up to Cancer is a division of the Entertainment Industry Foundation, and research grants are administered by the American Association for Cancer Research, the scientific partner of SU2C. Funding was also provided by Alex's Lemonade Stand Foundation for Childhood Cancer (R.A.G.); by the German Research Foundation (DFG, Deutsche Forschungsgemeinschaft; KU-2906/1-1 to A.K.); and by the National Center for Advancing Translational Sciences of the National Institutes of Health (U01TR002487 to A.L.W., W.H., R.A.G. and J.R.P.). The content is solely the responsibility of the authors and does not necessarily represent the official views of the National Institutes of Health.

Author contributions

N.A.V., A.J.J., A.L.W., J.K.Y., C.A.C., C.M.A., N.P., J.G., L.S.F., J.G.O., J.W., R.J.O., M.B., R.A.G., M.C.J. and J.R.P. participated in the design or interpretation of the reported experiments or results. N.A.V., A.J.J., A.L.W., C.B., J.K.Y., A.K., C.A.C., S.R.-R., W.H., K.S., M.B., M.C.J. and J.R.P. participated in the acquisition or analysis of data. N.A.V., A.J.J., A.L.W., M.C.J. and J.R.P. wrote the manuscript. M.C.J. and J.R.P. supervised all aspects of the research.

Competing interests

M.C.J. has interests in Umoja Biopharma and Juno Therapeutics, a Bristol Myers Squibb company. He is a seed investor and holds ownership equity in Umoja, serves as a member of the Umoja Joint Steering Committee and is a Board Observer of the Umoja Board of Directors. M.C.J. also holds patents, some of which are licensed to Umoja Biopharma and Juno Therapeutics. R.A.G. serves on a study steering committee for and is an inventor on a patent licensed to Juno Therapeutics and has served on advisory boards for Novartis. A.J.J. is an inventor on issued and pending patents related to CAR T cell therapies, and R.J.O. receives research support from Lentigen Technology, a Miltenyi Biotec company, and is a consultant for Umoja Biopharma. All other authors declare no competing financial interests.

Additional information

Extended data is available for this paper at https://doi.org/10.1038/s41591-021-01404-8.

Supplementary information The online version contains supplementary material available at https://doi.org/10.1038/s41591-021-01404-8.

Correspondence and requests for materials should be addressed to N.A.V.

Peer review information *Nature Medicine* thanks Arzu Onar-Thomas and the other, anonymous, reviewer(s) for their contribution to the peer review of this work. Saheli Sadanand was the primary editor on this article and managed its editorial process and peer review in collaboration with the rest of the editorial team.

Reprints and permissions information is available at www.nature.com/reprints.

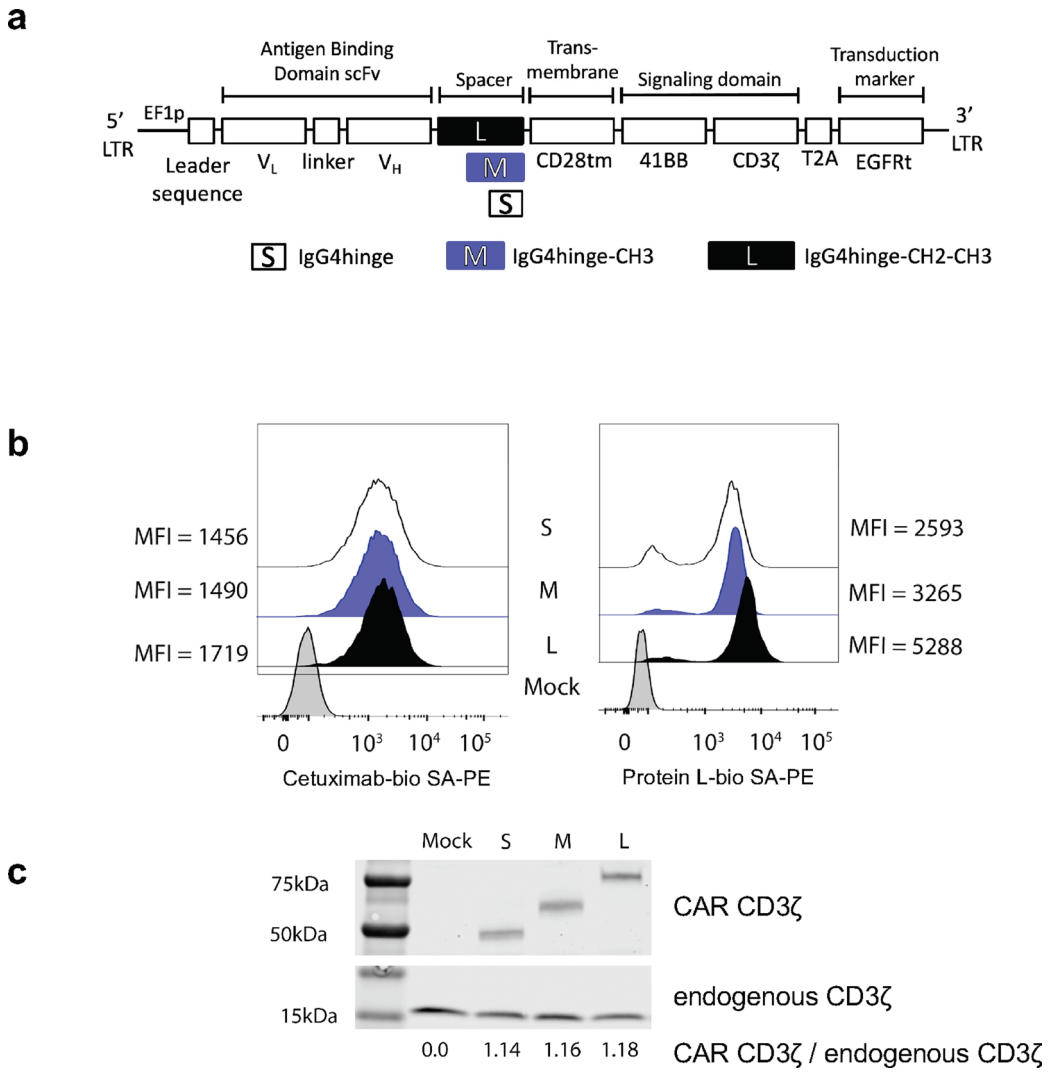

Extended Data Fig. 1 | HER2CAR spacer variants are efficiently expressed in CD8+ T cells. a, Schematic of 2nd generation HER2CAR extracellular domain spacer variants: Short (S), IgG4-hinge; Medium (M), IgG4-hinge-CH3; Long (L), IgG4-hinge-CH2-CH3. **b**, Human CD8 + T cell surface expression of S, M and L spacer variants of CAR T (EGFRt+) cells detected by cetuximab and Protein-L. **c**, CAR expression detected by CD3ζ-specific western blot. This experiment was performed in duplicate and a representative image is shown.

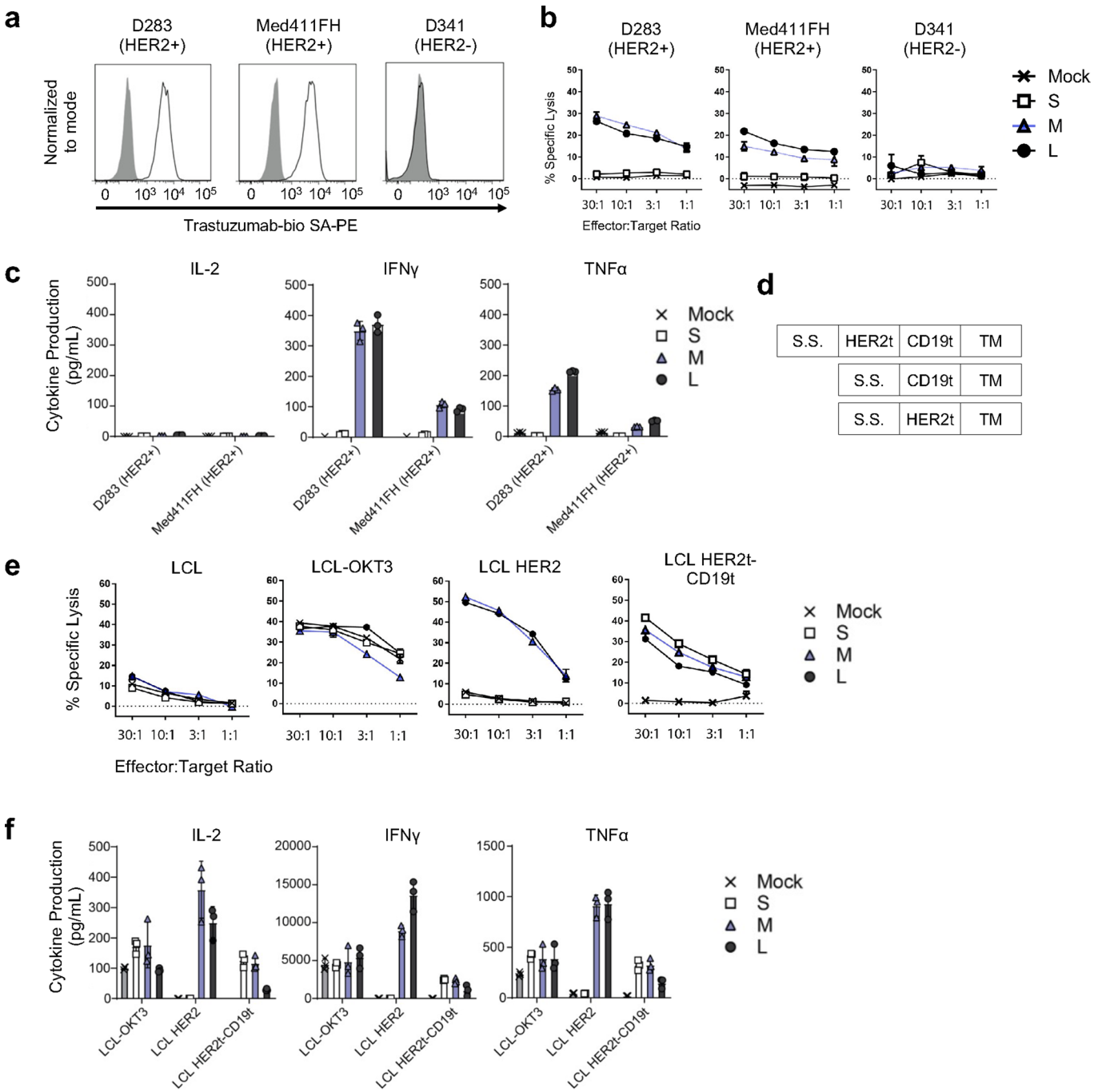

Extended Data Fig. 2 | HER2 epitope location influences HER2CAR T cell activity. a, Flow analysis of HER2+ (D283, Med411FH) and HER2- (D341) medulloblastoma cell lines. **b**, In vitro cytotoxicity of HER2-specific CAR T cells against target cell lines. **c**, Cytokine release assay of supernatants obtained from 24-hour co-cultures of CD8+ T cells expressing the HER2CAR extracellular spacer variants, with target cells at a 2:1 ratio. N = 3 technical replicates per condition and data presented as mean values +/− SD. **d**, Schematic of HER2t-CD19t components: In-frame fusion of GMCSFRss, HER2t (aa 563–653 of HER2) and CD19t (aa 20–323 of CD19). SS, signal sequence; TM, transmembrane domain. **e**, In vitro cytotoxicity of HER2-specific CAR T cells against a lymphoblastoid cell line (LCL) panel (parental, OKT3, HER2, and HER2t-CD19t). The x-axis shows the ratio of effector:target cells. **f**, Cytokine release assay of supernatants obtained from 24-hour co-cultures of CD8 + T cells expressing the HER2CAR extracellular spacer variants with LCL targets at a 2:1 ratio. N = 3 technical replicates per condition and data presented as mean values ± SD.

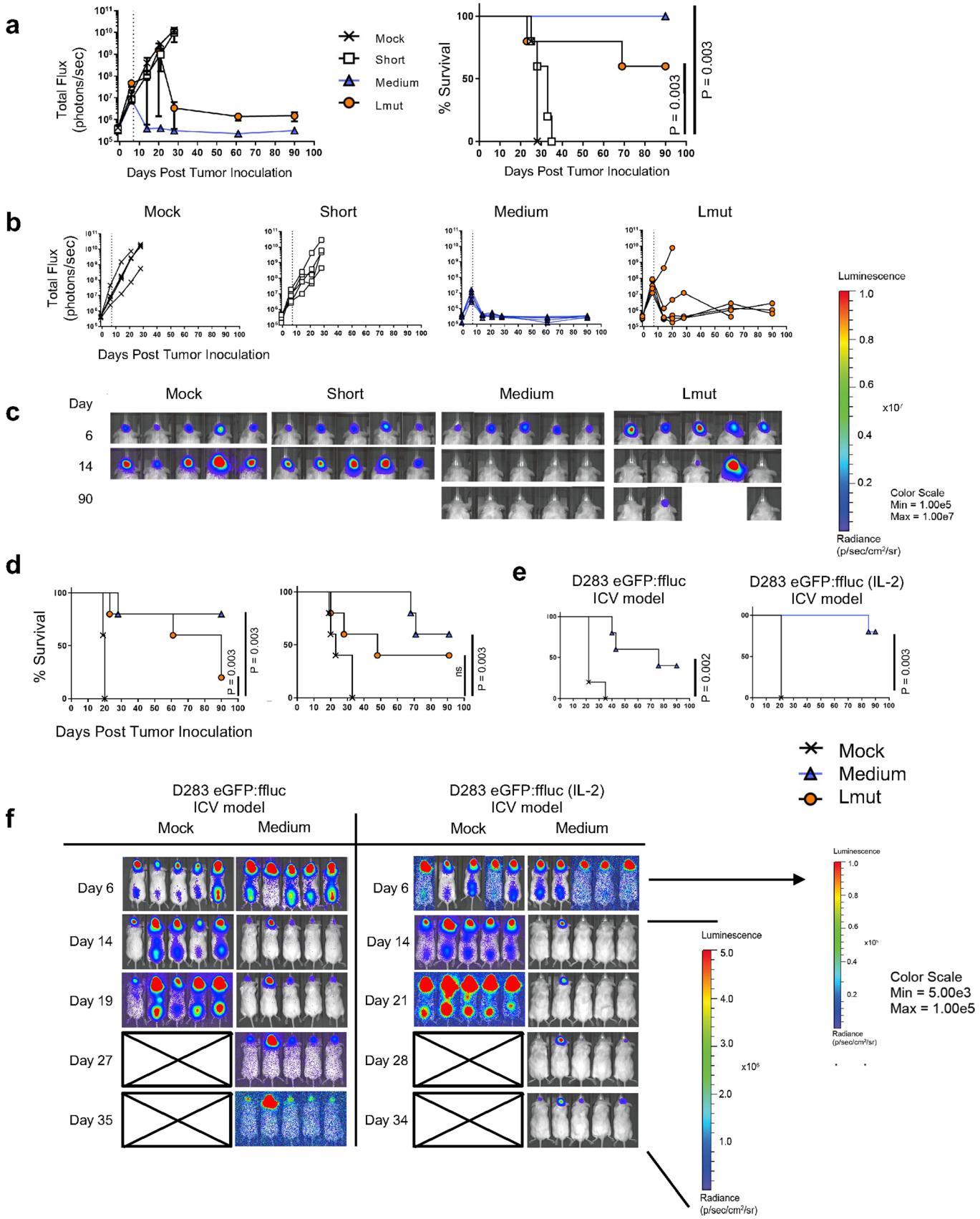

Extended Data Fig. 3 | See next page for caption.

Extended Data Fig. 3 | Medium-spacer HER2CAR T cells prolong survival and target metastases in an orthotopic xenograft model. Groups of mice were inoculated with 0.2e6 D283 eGFP:ffluc medulloblastoma cells (Day 0) and 2e6 HER2CAR CD8 + T cells (Day 7 – dotted vertical line) (**a-d**) intracranially or (**e**) via intracerebroventricular injection (ICV). **a,b**, Serial bioluminescence imaging of tumor in groups of mice treated with Mock, Short, Medium, or Lmut spacer HER2CAR CD8+ T cells. Data presented as mean values ± SD. N = 5 animals per group. All Kaplan-Meier statistical significance determined by one-sided log-rank (Mantel-Cox) test (M-spacer versus mock (P = 0.0035), S-spacer (P = 0.0021) and Lmut-spacer (P = 0.025). **c**, Bioluminescence imaging measured in region of interest (head) for orthotopic intracranial model. **d**, Kaplan-Meier analysis of survival in treatment (Medium and Lmut) and control (Mock) groups from repeat experiments. **e**, Kaplan-Meier analysis of survival in treatment and control groups of ICV dosed tumor models: D283 eGFP:ffluc cells (no IL-2) and D283 eGFP:ffluc cells (IL-2). **f**, Serial bioluminescence imaging in treatment and control groups of ICV dosed tumor models: D283 eGFP:ffluc cells (no IL-2) and D283 eGFP:ffluc cells (IL-2). All in vivo data are representative of a minimum of two independent experiments.

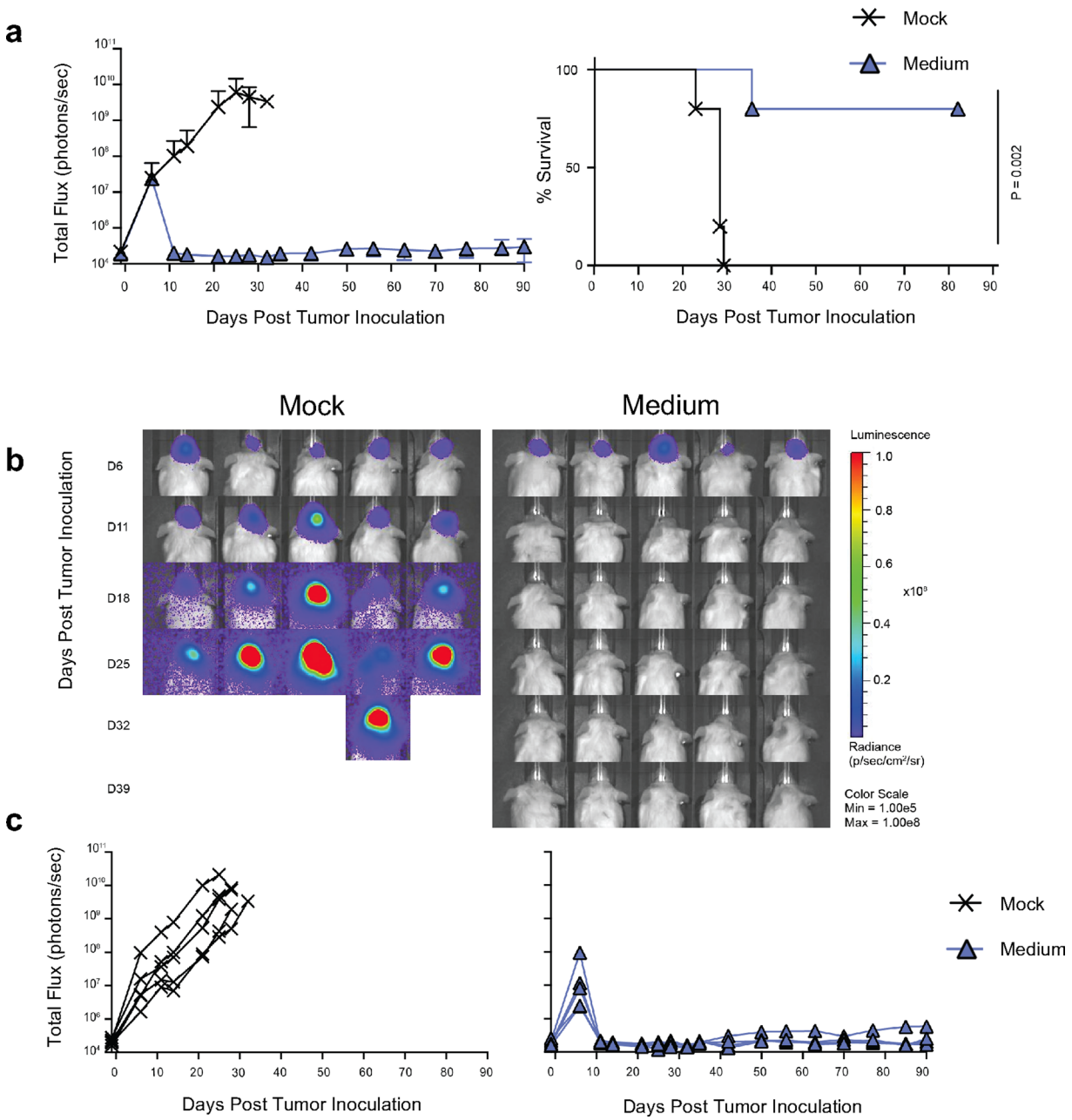

Extended Data Fig. 4 | HER2CAR T cells prolong survival in an intercranial xenograft model. a, NSG mice were injected with 2e6 mixed CD4+ :CD8+ HER2CAR T cells or un-transduced CD4+ :CD8+ Mock T cells 7 days post intracranial tumor inoculation with 0.2e6 D283 eGFP:ffluc medulloblastoma cells. Serial bioluminescence tumor imaging (left) and Kaplan-Meier analysis of survival (right) were performed. HER2CAR T cell treated mice survived significantly longer than the un-transduced Mock group (one-sided log-rank (Mantel-Cox) test, $p = 0.002$). Data presented as mean values ± SD. $N = 5$ animals per group. Bioluminescence images are from one representative experiment. **b**, Serial bioluminescence signal measured in region of interest (head) from mice treated with Mock or HER2CAR T cells. **c**, Individual serial bioluminescence imaging of tumor from un-transduced Mock (left) or HER2CAR T cell groups (right).

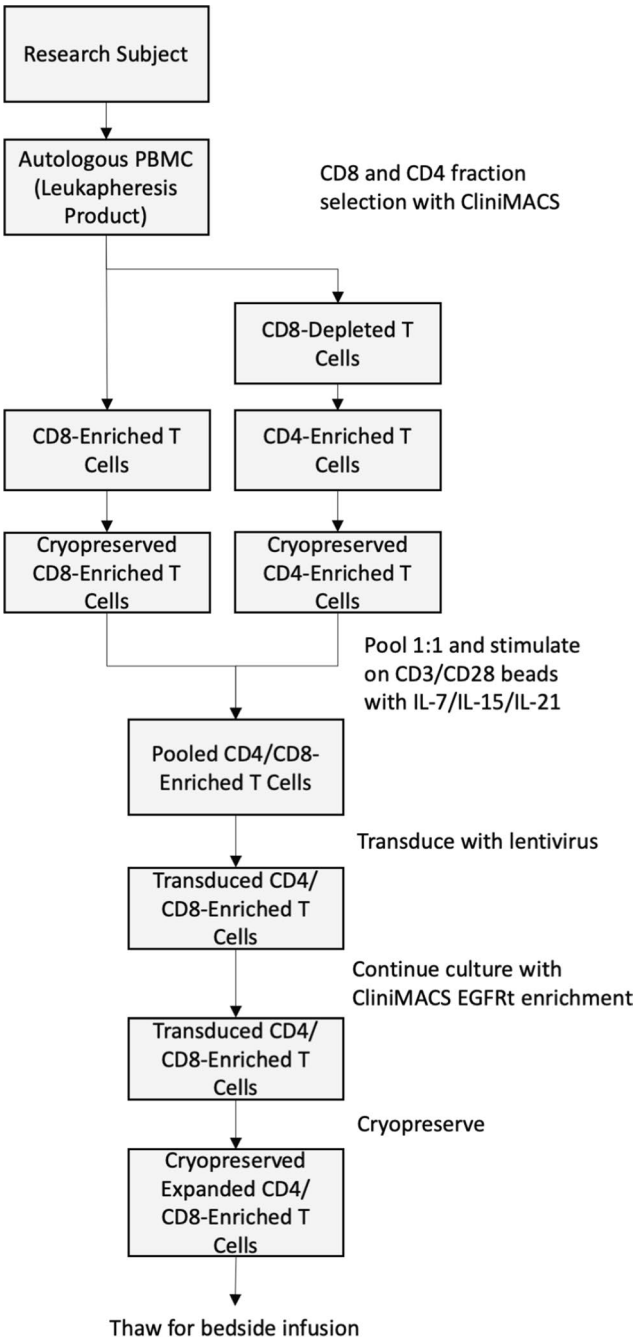

Extended Data Fig. 5 | Manufacturing schema for HER2CAR T cells. Flow diagram of the manufacturing process from apheresis to CAR T cell delivery.

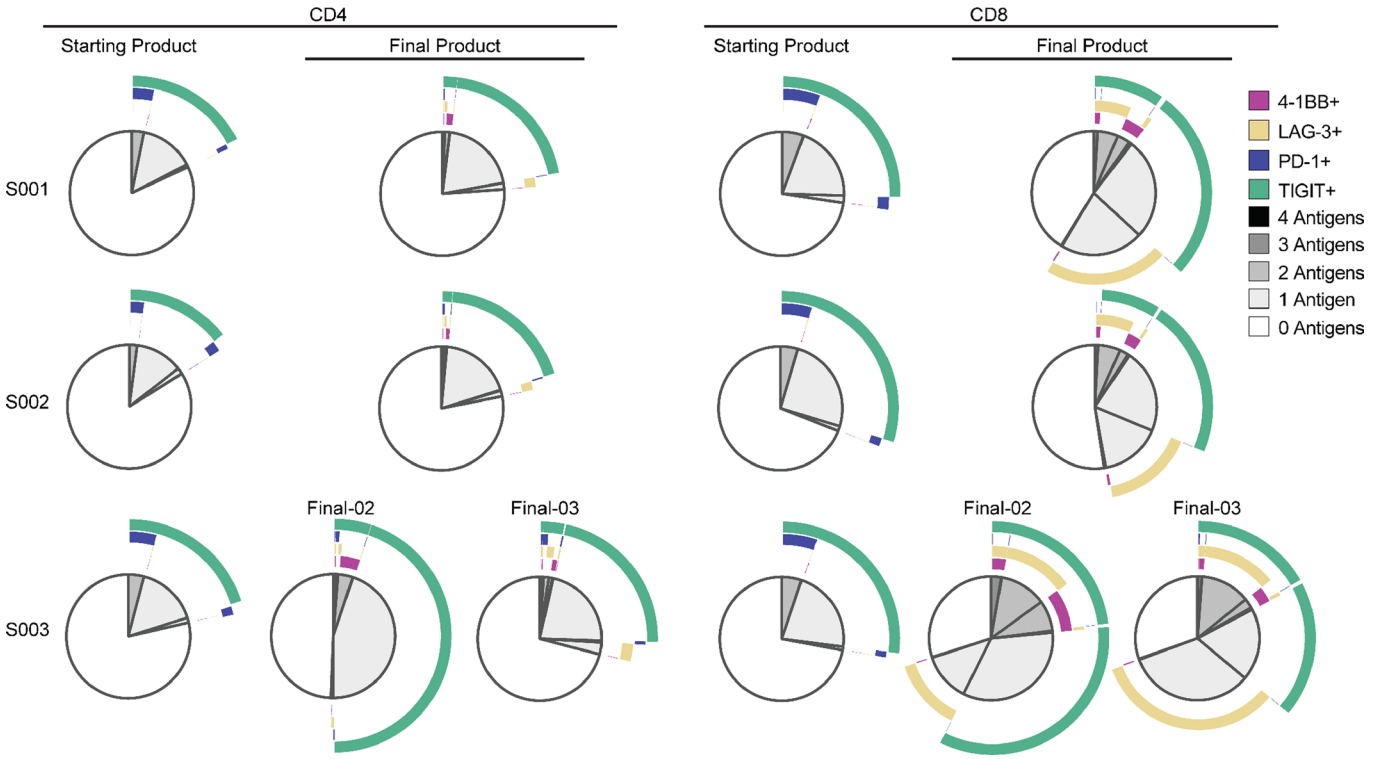

Extended Data Fig. 6 | Multiparameter co-expression profiles of activation/exhaustion markers for patient starting and final products. Boolean gating was performed for activation markers of interest before visualization via SPICE analysis software. Final-02 and Final-03 refer to second and third manufacturing attempts for S003. Two-sided permutation tests performed with 10,000 iterations per the built-in SPICE analysis function found no significant differences between samples ($p > 0.05$). Representative flow gating strategy shown in Supplementary Fig. 1a,b.

Extended Data Fig. 7, Table: Observed Toxicities (CTCAEv5.0)				
Subject	Body System Organ Class	Toxicity Type	Baseline Grade*	Maximum Grade
S001	EYE DISORDERS	Blurred vision		1
	GASTROINTESTINAL DISORDERS	Nausea	1	2
		Vomiting		2
	INJURY	Fall		1
	NERVOUS SYSTEM DISORDERS	Dysarthria		2
		Dysphasia		2
		Headache	1	2
		Muscle weakness, right-sided	1	2
		Proprioception decreased r foot r hand		2
		R foot dorsiflexion decreased		2
		Tremor		1
S002	GENERAL DISORDERS	Fatigue		1
		Fever		1
	NERVOUS SYSTEM DISORDERS	Headache		3
		Lower back pain		2
	SKIN AND SUBCUTANEOUS TISSUE DISORDERS	Goosebumps		1
S003	GASTROINTESTINAL DISORDERS	Nausea		1
		Vomiting		1
	GENERAL DISORDERS	Chills		1
		Fever		3
	INVESTIGATIONS	Lymphocyte count decreased	2	2
	MUSCULOSKELETAL	Back pain	2	3
	NERVOUS SYSTEM DISORDERS	Headache		3
		Peripheral sensory neuropathy		1
		Tremor		1
	SKIN AND SUBCUTANEOUS TISSUE DISORDERS	Scalp pain		1
	VASCULAR DISORDERS	Hypotension		1

*(if present at pre course 1 week 1 dose administration)

Extended Data Fig. 7 | Observed toxicities. CTCAE grading of all observed toxicities that constituted an increase from baseline. If the toxicity was not present pre-Course 1 Week 1 administration, then no baseline grade is shown.

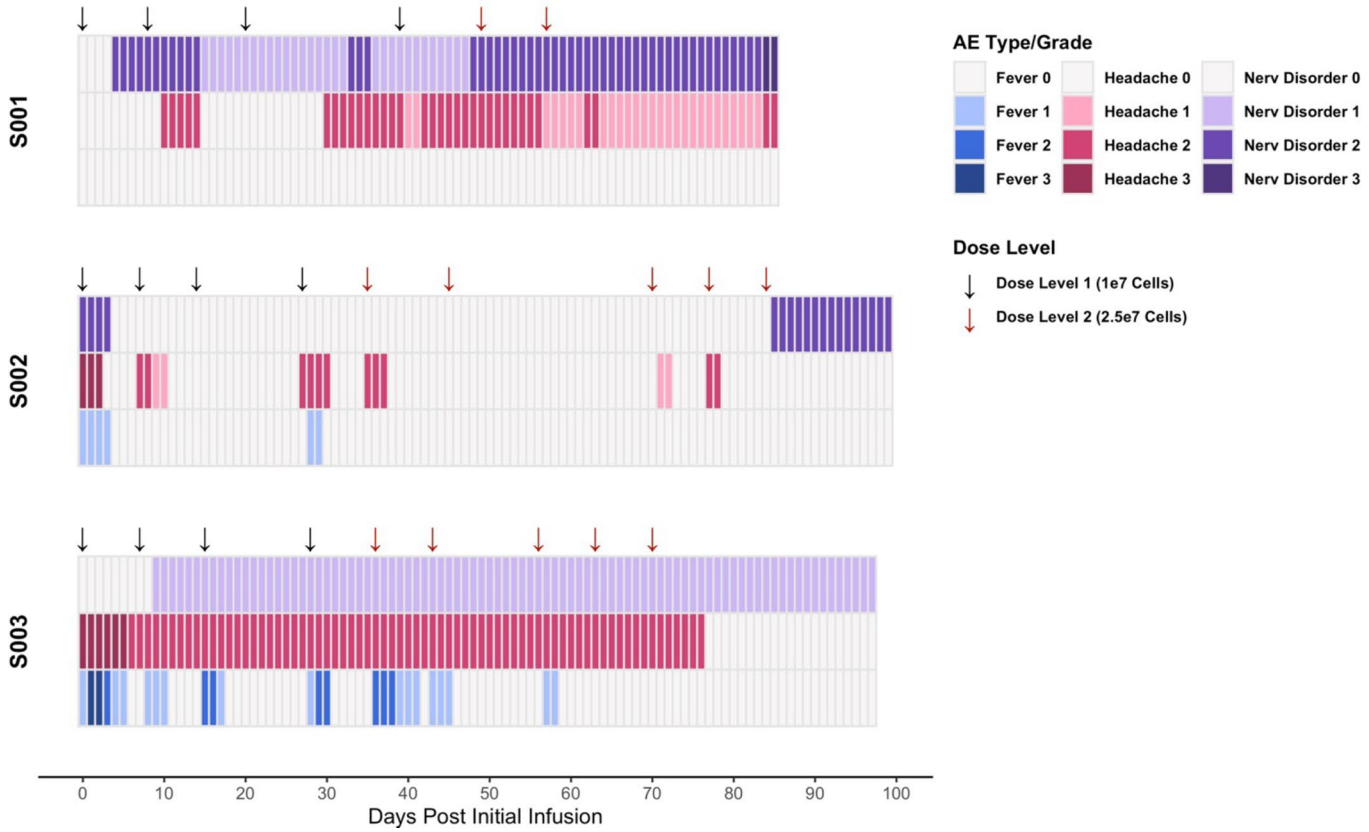

Extended Data Fig. 8 | Adverse event development over the course of treatments. Three adverse event (AE) types are plotted here: fever, headaches, and nervous system disorders (excluding headache). CAR T cell infusions indicated with arrows.

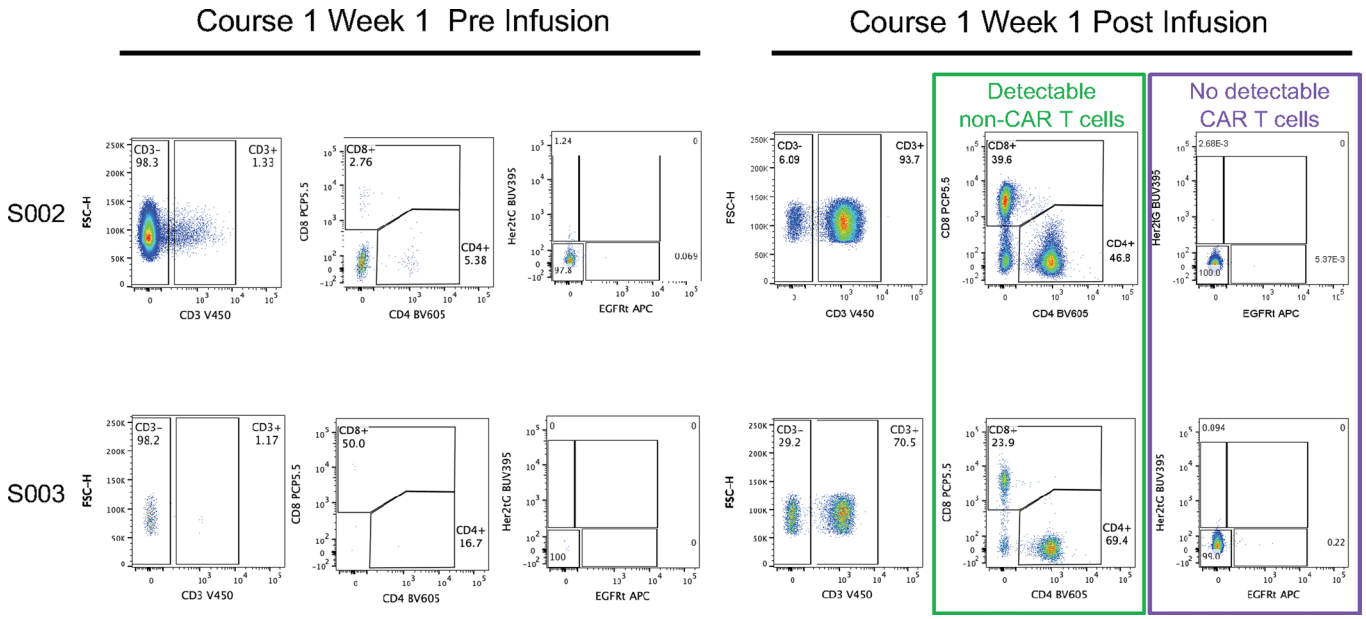

Extended Data Fig. 9 | Pre versus post infusion detection of T cell populations in CSF via flow cytometry. Representative pre and post infusion flow plots from S002 and S003 show no detectable CAR T (EGFRt+) cells, but detectable non-CAR T cells (both CD4+ and CD8+ T cells) in subject CSF post infusion. Representative flow gating strategy shown in Supplementary Fig. 1d.

nature research

Corresponding author(s): Nicholas Vitanza

Last updated by author(s): 05/17/2021

Reporting Summary

Nature Research wishes to improve the reproducibility of the work that we publish. This form provides structure for consistency and transparency in reporting. For further information on Nature Research policies, see Authors & Referees and the Editorial Policy Checklist.

Statistics

For all statistical analyses, confirm that the following items are present in the figure legend, table legend, main text, or Methods section.

n/a	Confirmed	
☐	☒	The exact sample size (*n*) for each experimental group/condition, given as a discrete number and unit of measurement
☐	☒	A statement on whether measurements were taken from distinct samples or whether the same sample was measured repeatedly
☐	☒	The statistical test(s) used AND whether they are one- or two-sided *Only common tests should be described solely by name; describe more complex techniques in the Methods section.*
☒	☐	A description of all covariates tested
☐	☒	A description of any assumptions or corrections, such as tests of normality and adjustment for multiple comparisons
☐	☒	A full description of the statistical parameters including central tendency (e.g. means) or other basic estimates (e.g. regression coefficient) AND variation (e.g. standard deviation) or associated estimates of uncertainty (e.g. confidence intervals)
☐	☒	For null hypothesis testing, the test statistic (e.g. *F*, *t*, *r*) with confidence intervals, effect sizes, degrees of freedom and *P* value noted *Give P values as exact values whenever suitable.*
☒	☐	For Bayesian analysis, information on the choice of priors and Markov chain Monte Carlo settings
☒	☐	For hierarchical and complex designs, identification of the appropriate level for tests and full reporting of outcomes
☒	☐	Estimates of effect sizes (e.g. Cohen's *d*, Pearson's *r*), indicating how they were calculated

Our web collection on statistics for biologists contains articles on many of the points above.

Software and code

Policy information about availability of computer code

Data collection	BD Fortessa II, Ivis Spectrum, Bio-Plex 200, Li-COR Odyssey Clx, TopCount Scintillation Counter
Data analysis	FlowJo v.10, Prism v.7, Living Image v.4.5.2, Image Studio v3.1, TopCount NXT v.3.01 , SPICE v6, R v3.6.3 with ggplot2 library v3.3.0.

For manuscripts utilizing custom algorithms or software that are central to the research but not yet described in published literature, software must be made available to editors/reviewers. We strongly encourage code deposition in a community repository (e.g. GitHub). See the Nature Research guidelines for submitting code & software for further information.

Data

Policy information about availability of data

All manuscripts must include a data availability statement. This statement should provide the following information, where applicable:

- Accession codes, unique identifiers, or web links for publicly available datasets
- A list of figures that have associated raw data
- A description of any restrictions on data availability

All requests for raw and analyzed data and materials will be promptly reviewed by the intellectual property office of Seattle Children's Research Institute to verify if the request is subject to any intellectual property or confidentiality obligations. Raw preclinical and clinical data is stored at Seattle Children's with indefinite appropriate backup. The full raw Western blot is shown in Supplemental Fig. 3. Patient-related data not included in the paper were generated as part of clinical trials and may be subject to patient confidentiality. Any data and materials that can be shared will be released via a Material Transfer Agreement.

Field-specific reporting

Please select the one below that is the best fit for your research. If you are not sure, read the appropriate sections before making your selection.

☒ Life sciences ☐ Behavioural & social sciences ☐ Ecological, evolutionary & environmental sciences

For a reference copy of the document with all sections, see nature.com/documents/nr-reporting-summary-flat.pdf

Life sciences study design

All studies must disclose on these points even when the disclosure is negative.

Sample size	See figures for replicates chosen. Power analysis (0.8) suggests that the experiments will have to use use 5-10 mice to detect significant difference of 10-20% with an error of 5%. The key endpoints for our experiments are: • Engraftment, persistence, and/or proliferation of CAR T cells • Regression or total eradication (positive treatment effect) or progression (negative control and/or no treatment effect) of engrafted tumor cells when adoptive immunotherapy is administered. Studies are designed to include the appropriate numbers of animals as needed to achieve statistical relevance and might be adjusted as a result of ongoing data collection. Our experience obtained with ex vivo generated CAR T cells therapies suggests that 5-10 mice per group will be required to make robust conclusions. This spread in required number of animals is due to known variations in engraftment characteristics between tumor types that we plan to study.
Data exclusions	No data were excluded from analysis.
Replication	Multiple biological replicates were used. Preclinical experiments were repeated at least 1 in a different cell donor. Attempts at experimental replication were successful.
Randomization	Mice were divided into groups following tumor engraftment. Average tumor flux and range values were the same between each group prior to T cell injection. No other measurements, such as mouse weight, were pursued.
Blinding	Investigators were otherwise not blinded. We do not have proper staff numbers to be able to blindly administer treatment or blindly collect data.

Reporting for specific materials, systems and methods

We require information from authors about some types of materials, experimental systems and methods used in many studies. Here, indicate whether each material, system or method listed is relevant to your study. If you are not sure if a list item applies to your research, read the appropriate section before selecting a response.

Materials & experimental systems

n/a	Involved in the study
☐	☒ Antibodies
☐	☒ Eukaryotic cell lines
☒	☐ Palaeontology
☐	☒ Animals and other organisms
☐	☒ Human research participants
☐	☒ Clinical data

Methods

n/a	Involved in the study
☒	☐ ChIP-seq
☐	☒ Flow cytometry
☒	☐ MRI-based neuroimaging

Antibodies

Antibodies used	CD3 (BD Biosciences Cat# 562426, RRID:AB_11152082 or BD Biosciences Cat# 652356, RRID:AB_2868395), CD4 (BD Biosciences Cat# 562658, RRID:AB_2744420), CD8a (BD Biosciences Cat# 560662, RRID:AB_1727513), CD36 (BD Biosciences Cat# 555454, RRID: AB_2291112), CD25 (BD Biosciences Cat# 564034, RRID:AB_2738556), CD27 (BD Biosciences Cat# 564301, RRID:AB_2744350), CD39 (BioLegend Cat# 328212, RRID:AB_2099950), CD45RA (BD Biosciences Cat# 563870, RRID:AB_2738459), CD45RO (BD Biosciences Cat# 564291, RRID:AB_2744410), CD95 (BD Biosciences Cat# 561633, RRID:AB_10894384), CD127 (BD Biosciences Cat# 563324, RRID:AB_2738138), CD137 (BioLegend Cat# 309820, RRID:AB_2563830), CCR4 (BioLegend Cat# 359410, RRID:AB_2562431), CCR6 (BD Biosciences Cat# 563704, RRID:AB_2738381), CCR7 (BD Biosciences Cat# 552176, RRID:AB_394354), CCR10 (BD Biosciences Cat# 563656, RRID:AB_2738351), CXCR3 (BD Biosciences Cat# 565223, RRID:AB_2687488), FoxP3 (BD Biosciences Cat# 560045, RRID:AB_1645411), LAG-3 (BioLegend Cat# 369310, RRID:AB_2629753), Nur77 (Thermo Fisher Scientific Cat# 12-5965-82, RRID:AB_1257209), PD-1 (BD Biosciences Cat# 565299, RRID:AB_2739167), TCRab (BD Biosciences Cat# 564725, RRID:AB_2738918), TCRgd (BD Biosciences Cat# 655434, RRID:AB_2827402), TIGIT (BioLegend Cat# 372712, RRID:AB_2632927), and TIM-3 (BioLegend Cat# 345032, RRID:AB_2565833). cetuximab (Creative Diagnostics Cat# TAB-003, RRID:AB_2459632) custom-conjugated to allophycocyanin by BD Biosciences; anti-CD247 (CD3ζ, BD Biosciences Cat #551033)

Validation	Cetuximab-APC and biotinylated Cetuximab and Trastuzumab antibodies were custom-conjugated by BD and validated in-house by flow cytometry. Titration experiments were performed using EGFR or HER2 expressing H9 cell lines or T cells transduced with research-grade vectors representative of other clinical trials managed by Seattle Children's. Trastuzumab staining is used as a part of the high-throughput system utilized by the Correlative Studies for analysis of all clinical trial samples, but only the trastuzumab negative populations were examined for specimens in this trial/manuscript. All other antibodies are validated in a similar way via positive staining on cell lines by flow cytometry mirroring manufacture validation.

Eukaryotic cell lines

Policy information about cell lines

Cell line source(s)	239T cells (ATCC CRL-3216), TM-LCL (gift from City of Hope), LCL-OKT3, HER2, Her2t-CD19t (made in house), D283 (ATCC HTB-185), Med411FH (gift from Jim Olson - Fred Hutchinson Cancer Research Center), D341 (ATCC HTB-187)
Authentication	All primary cell lines authenticated by the University of Arizona Genetics core by STR (short tandem repeat) profiling, matched to the DSMZ Database (Deutsche Sammlung von Mikroorganism un Zellkulturen https://www.dsmz.de/), with the exception of the Med411FH and TM-LCL, immortalized patient lines. TM-LCL and Med411FH cell lines were also profiled by STR profiling, however because they are patient derived cell lines there is no reference to match them too.
Mycoplasma contamination	All cell lines tested negative for mycoplasma contamination.
Commonly misidentified lines (See ICLAC register)	No commonly misidentified cell lines were used in the study.

Animals and other organisms

Policy information about studies involving animals; ARRIVE guidelines recommended for reporting animal research

Laboratory animals	10-12 week old male NOD.Cg-PrkdcscidIL2rgtm1Wjl/SzJ (NSG) mice were used in this study. Mice from each cohort were housed together in individually ventilated cages at a temperature of 68-78F, humidity of 40-70%, 10-15 air changes per hour, and a 12 hour light cycle with lights on at 7:00 AM.
Wild animals	This study did not involve wild animals.
Field-collected samples	This study did not involve field-collected animals.
Ethics oversight	All mouse experiments were conducted under protocols approved by the Seattle Children's Research Institute's Institutional Animal Care and Use Committee.

Note that full information on the approval of the study protocol must also be provided in the manuscript.

Human research participants

Policy information about studies involving human research participants

Population characteristics	The three BrainChild-01 patients (S001, S002 and S003) described in this initial report were enrolled on DR1 of their respective Arm (Table 1). All patients had undergone three or more tumor-directed surgical procedures and had received at least 1 prior irradiation and at least 1 prior chemotherapy regimen. Prior to opening enrollment to ages 1 through 26 years, we enrolled a cohort aged 15 through 26 years as they could more readily self-report any neurologic changes. The first three patients were 19 (F), 16 (M), and 26 (M) years of age but at the time of tumor diagnosis all patients were of pediatric age with presumed pediatric biology of their tumors.
Recruitment	In unbiased fashion irrespective of gender or other physical or social attributes, but requiring appropriate age and tissue staining criteria, subjects with progressive disease were made aware of the trial either internally at Seattle Childrens through direct communication with our neuro-oncology team or at external sites by neuro-oncologists aware of our trial opening, and patients who met eligibility were enrolled in the order in which they contacted our program for potential enrollment. All patients who met eligibility were offered the trial.
Ethics oversight	Seattle Children's Institutional Review Board

Note that full information on the approval of the study protocol must also be provided in the manuscript.

Clinical data

Policy information about clinical studies

All manuscripts should comply with the ICMJE guidelines for publication of clinical research and a completed CONSORT checklist must be included with all submissions.

Clinical trial registration	NCT03500991

Study protocol	The full clinical trial protocol is not included as it contains proprietary information and the trial is still open and accruing patients.
Data collection	Clinical data is collected at Seattle Childrens, the single site of the clinical trial NCT0350091.
Outcomes	The primary objectives of this study are to assess the feasibility, safety, and tolerability of CNS locoregional adoptive therapy with autologous CD4+ and CD8+ T cells lentivirally transduced to express a HER2-specific CAR and EGFRt, delivered by an indwelling catheter in the tumor cavity or ventricular system, in children and young adults with recurrent/refractory HER2-positive CNS tumors. Feasibility is defined as generating sufficient therapeutic product to receive a minimum of 6 doses at the intended DL per assigned dose regimen, after two attempts using a single apheresis product for starting material. Safety and tolerability are determined by data that include history/physical exams, laboratory/radiographic evaluations, and Common Terminology Criteria for Adverse Events (CTCAE v5.0). A dose limiting toxicity (DLT) is defined as an event which, in the opinion of the investigator, is possibly, probably, or definitely attributable to the CAR T product and which occurs from the time of initial CAR T cell infusion through 28 days following the final CAR T cell infusion. A DLT includes all ≥ grade 3 CTCAE v5.0 toxicities except ≥ grade 3 toxicities that are known to be related to CAR T cells, including grade 4 CRS that decreases to ≤ grade 2 within 72 hours; grade 3 CRS that decreases to ≤ grade 2 within 7 days; ≥ grade 3 hypotension, fever, and/or chills not controlled with medical intervention that decrease to ≤ grade 2 within 72 hours; ≥ grade 3 activated PTT, fibrinogen, and/or INR that are asymptomatic and resolve within 72 hours; ≥ grade 3 hypoglycemia and/or electrolyte imbalance that are asymptomatic and resolve within 72 hours; ≥ grade 3 nausea and/or vomiting that decrease to ≤ grade 2 with 7 days; and ≥ grade 3 neurologic symptoms that decrease to ≤ grade 2 with 7 days. The definition of a DLT also includes any toxicity lasting > 14 days that prevents the patient from meeting criteria for subsequent CAR T cell infusion. Secondary objectives of this study are to assess CAR T cell distribution within the CSF and the extent to which CAR T cells egress to the peripheral circulation, as measured by serum qPCR; to assess whether HER2 expression changes in relapsed CNS tumors that were HER2-positive prior to treatment with CAR T cells, as measured by immunohistochemistry; and to assess disease response to HER2-specific CAR T cell CNS-directed therapy, as measured by neuroimaging and clinical course. Patients are assigned a neurotoxicity score at each clinical evaluation during protocol therapy. Toxicity grade ranges from 0-5: (0) is normal or no change from baseline examination at the start of therapy; (1) is mild lethargy and/or irritability or visual, motor, or sensory symptoms without change in neurological exam; (2) is moderate lethargy, disorientation, or psychosis lasting less than 48 hours, or mild increase in preexisting neurological deficit; (3) is greater than 48 hours of severe lethargy, responsiveness to verbal stimuli, disorientation or psychosis lasting greater than 48 hours, moderate increase in preexisting neurological deficit or the onset of new neurological signs, or greater than two seizures in 24 hours; (4) is coma, unresponsive to verbal stimuli, increasing neurologic deficit > grade 3, evidence of herniation, development of uncontrolled seizures, intracerebral hemorrhage; (5) is death.

Flow Cytometry

Plots

Confirm that:

☒ The axis labels state the marker and fluorochrome used (e.g. CD4-FITC).

☒ The axis scales are clearly visible. Include numbers along axes only for bottom left plot of group (a 'group' is an analysis of identical markers).

☒ All plots are contour plots with outliers or pseudocolor plots.

☒ A numerical value for number of cells or percentage (with statistics) is provided.

Methodology

Sample preparation	Adherent cells were trypsinized, spun down and resuspended in PBS. Nonadherent cells were resuspended in PBS.
Instrument	LSRII Fortessa (BD Biosciences) or MACSQuant (Miltenyi Biotec)
Software	FlowJo V10.5.3
Cell population abundance	Refer to histograms/% on figures.
Gating strategy	CAR T cells were defined as singlets/lymphocytes/viableCD36-/CD3+/EGFRt+/CD4+ or CD8+. In general, markers of interest were examined in the EGFRt-negative or EGFRt-positive populations as applicable for starting or final product samples, with the exception of CD25, CD127, FoxP3, TCRab, and TCRgd. These markers were stained in a flow cytometry panel that did not include EGFRt selection and are therefore reported as a percentage of the total CD4+ or CD8+ population. Multi-activation marker profiles were analyzed via Boolean gating and SPICE analysis software. Representative flow gating is in Supp. Fig. 1.

☒ Tick this box to confirm that a figure exemplifying the gating strategy is provided in the Supplementary Information.